

Supplementary materials for the article “ R^2D^2 : Accounting for temporal dependences in multivariate bias correction via analogue ranks resampling”

Mathieu Vrac and Soulivanh Thao

Laboratoire des Sciences du Climat et de l'Environnement (LSCE-IPSL), CEA/CNRS/UVSQ, Université Paris-Saclay
Centre d'Etudes de Saclay, Orme des Merisiers, 91191 Gif-sur-Yvette, France

Correspondence: Mathieu Vrac (mathieu.vrac@lsce.ipsl.fr)

5

10

15

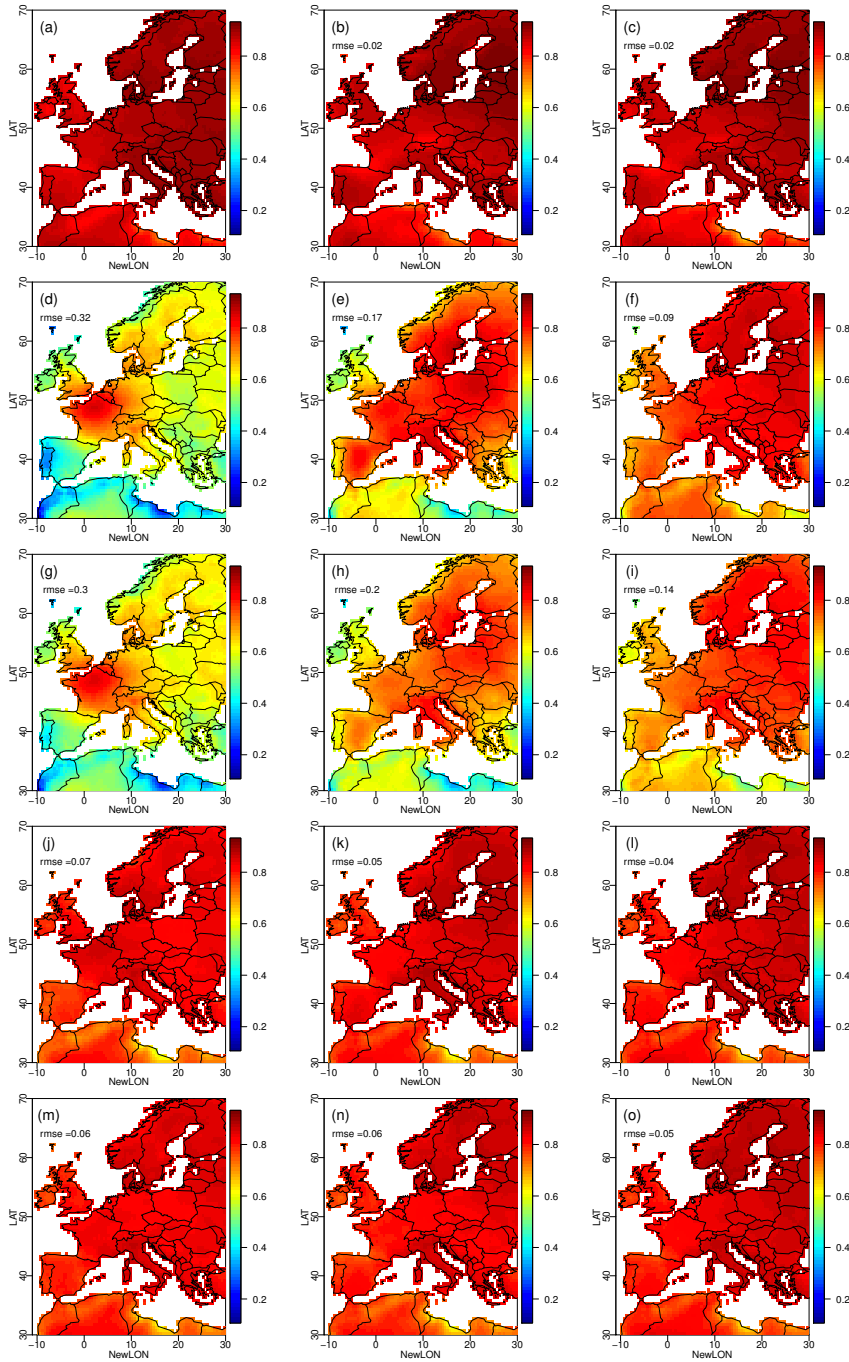


Figure 1. Maps of order 1-day temperature autocorrelations for Spring over the 1979-2016 period, for (a) WFDEI, (b) IPSL raw simulations, (c) 1d-bias correction (CDF-t), (d) R.1.1.0, (e) R.5.1.0, (f) R.100.1.0, (g) R.1.2.0, (h) R.5.2.0, (i) R.100.2.0, (j) R.1.1.1, (k) R.5.1.1, (l) R.100.1.1, (m) R.1.2.1, (n) R.5.2.1, (o) R.100.2.1. In other words, 2nd row: results for temperature as reference variable (for different numbers of locations) and with no lags accounted for; 3rd row: same but for temperature and precipitation together as reference variable; 4th and 5th rows: same as 2nd and 3rd but with lags accounted for. For (b-o), the RMSE value, computed over the whole domain between WFDEI autocorrelations and those from the model or corrected data, is indicated.

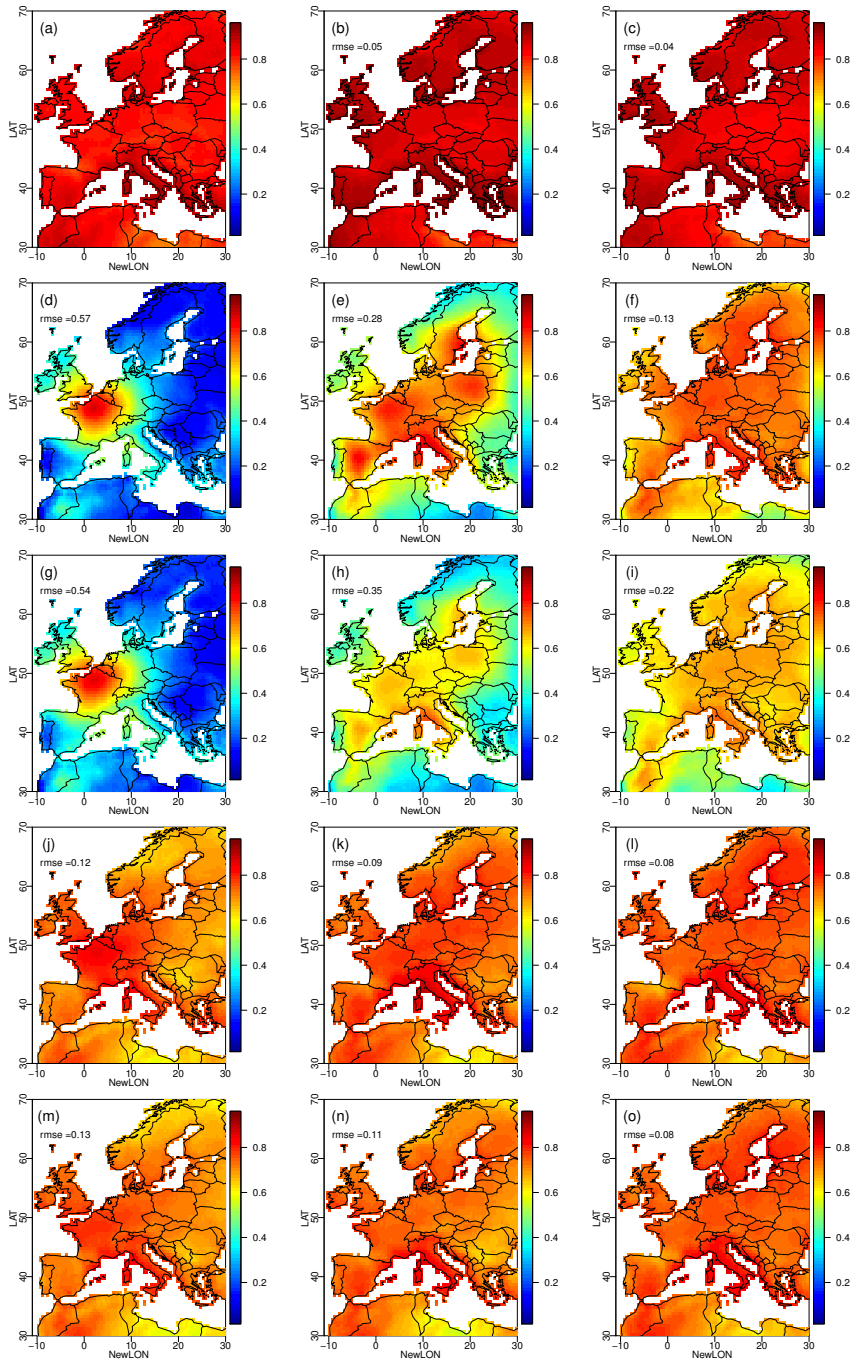


Figure 2. Same as Figure SM1 but for Summer temperature autocorrelations.

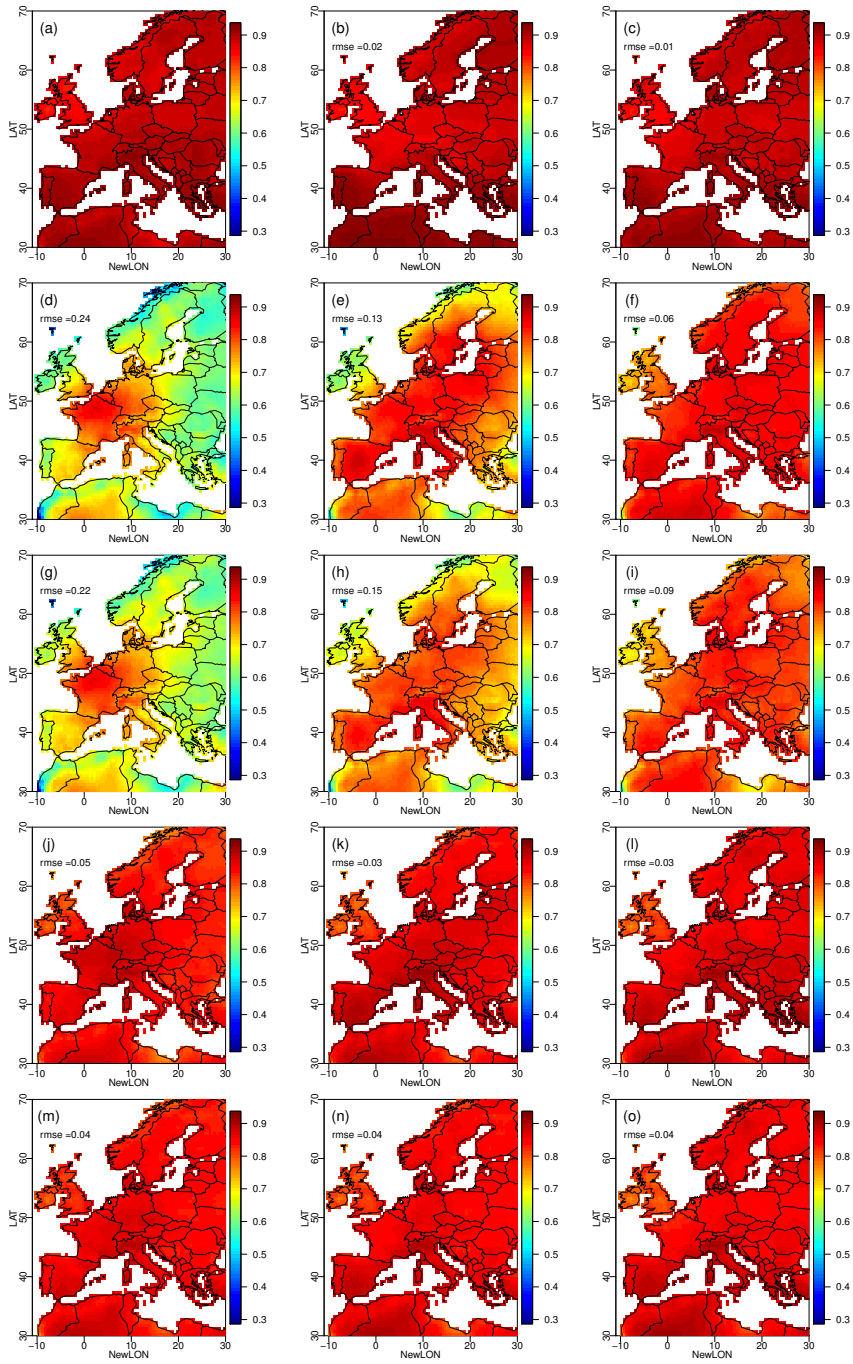


Figure 3. Same as Figure SM1 but for fall temperature autocorrelations.

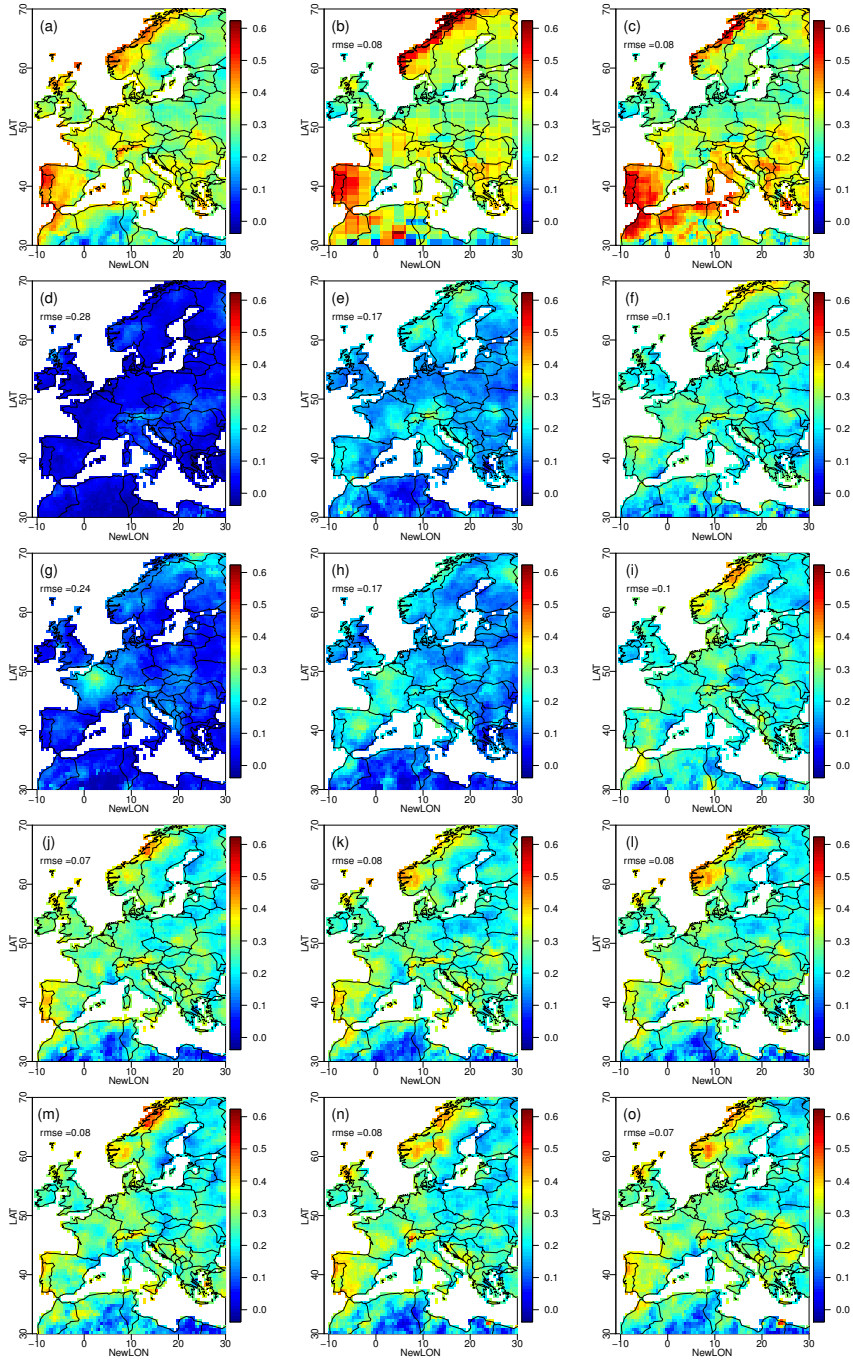


Figure 4. Same as Figure SM1 but for Spring precipitation autocorrelations.

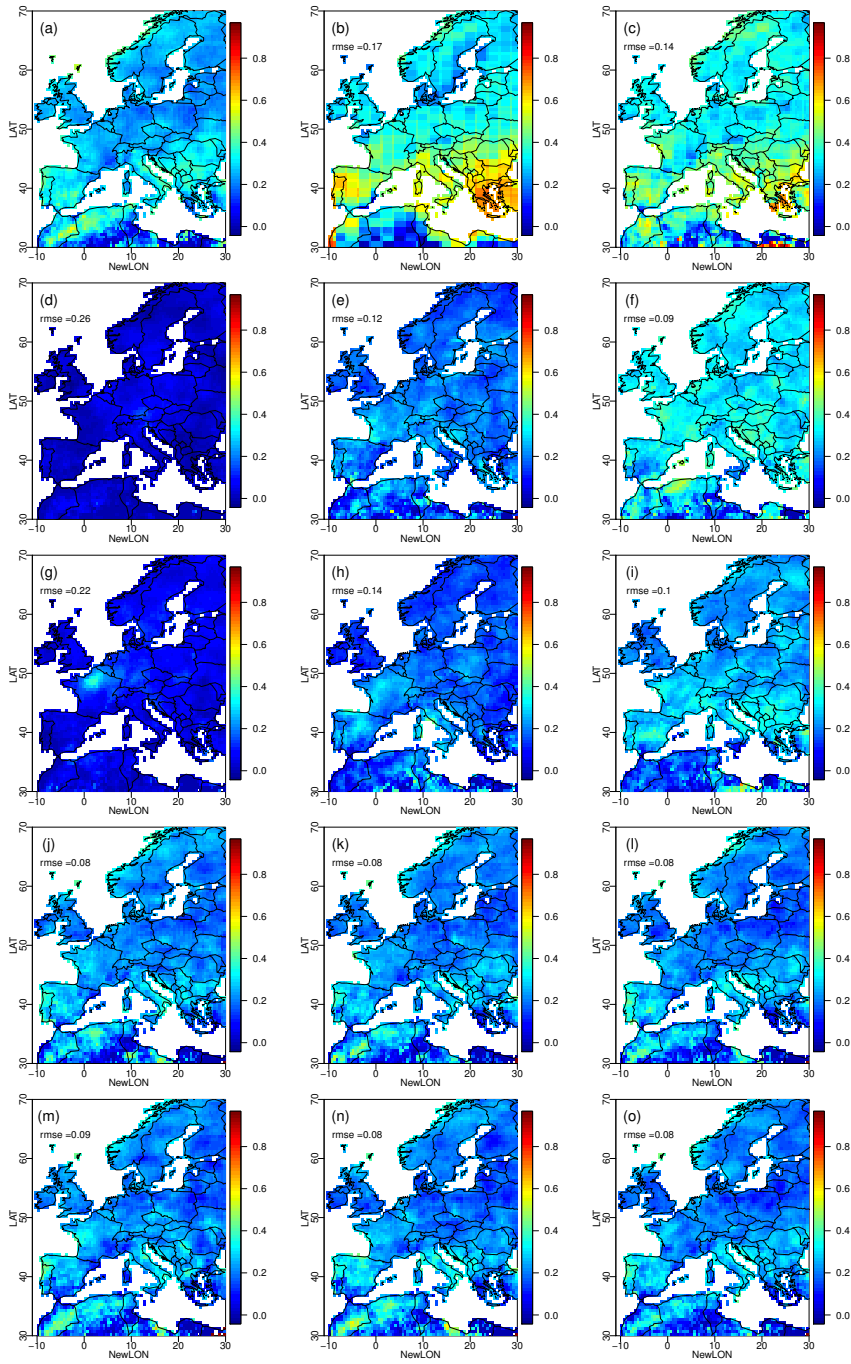


Figure 5. Same as Figure SM1 but for Summer precipitation autocorrelations.

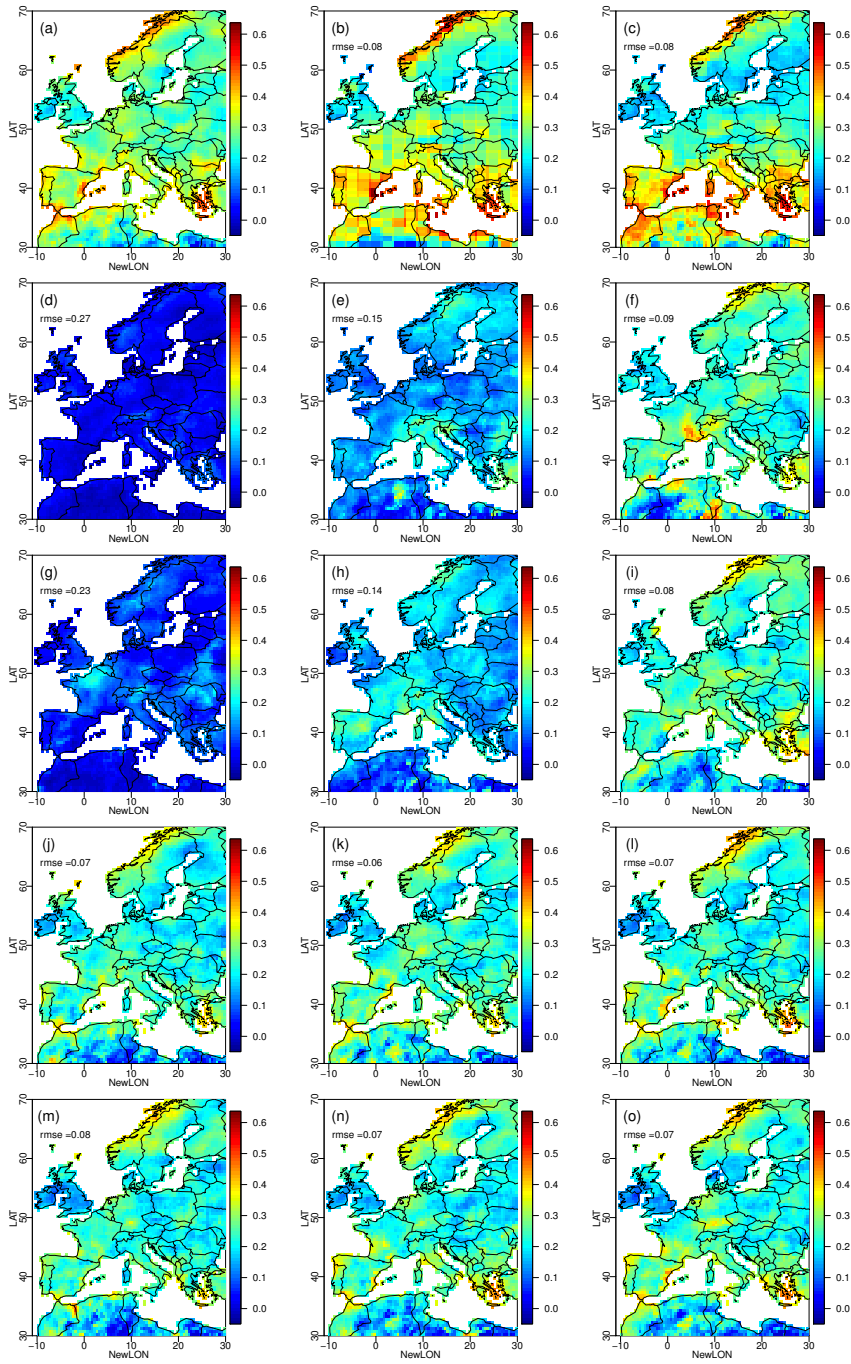


Figure 6. Same as Figure SM1 but for Fall precipitation autocorrelations.

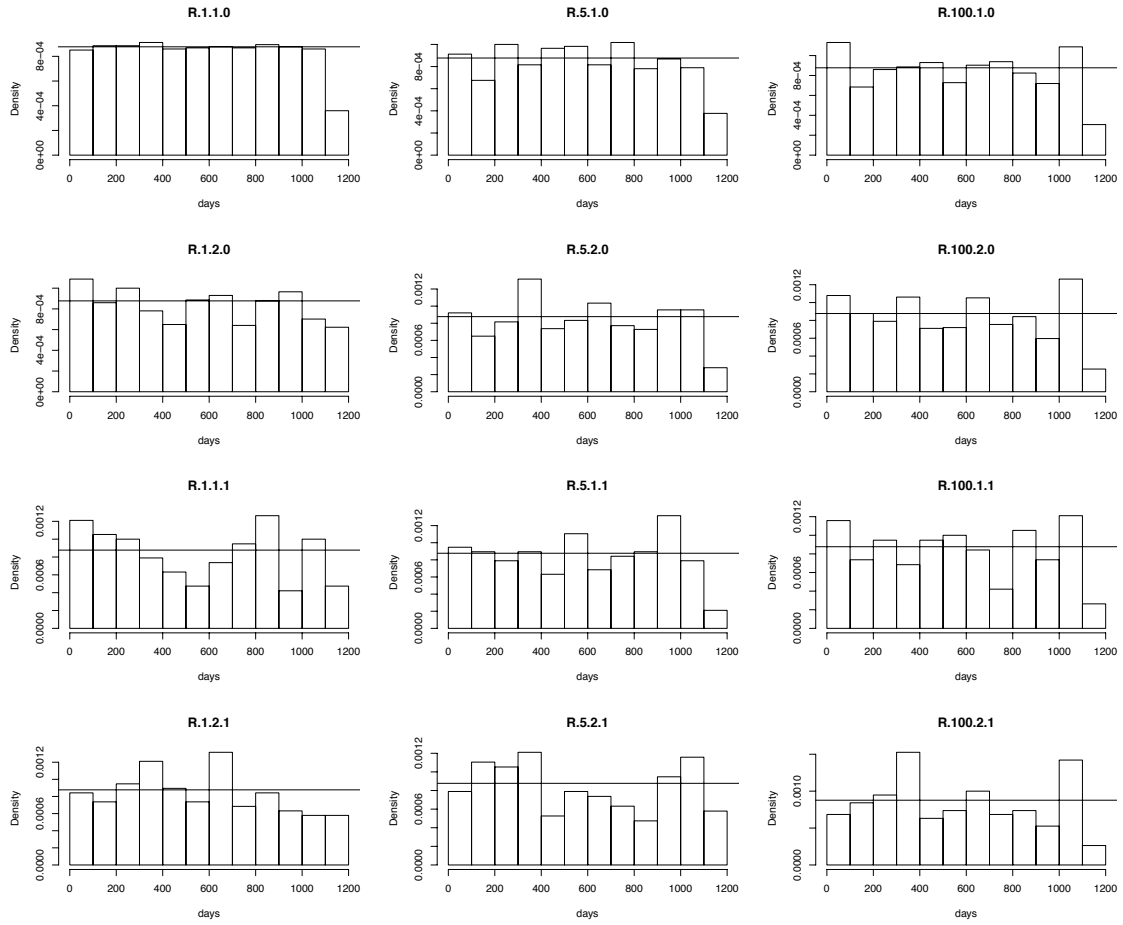


Figure 7. Distributions of time steps selected in the reference dataset in April by the different R^2D^2 configurations.

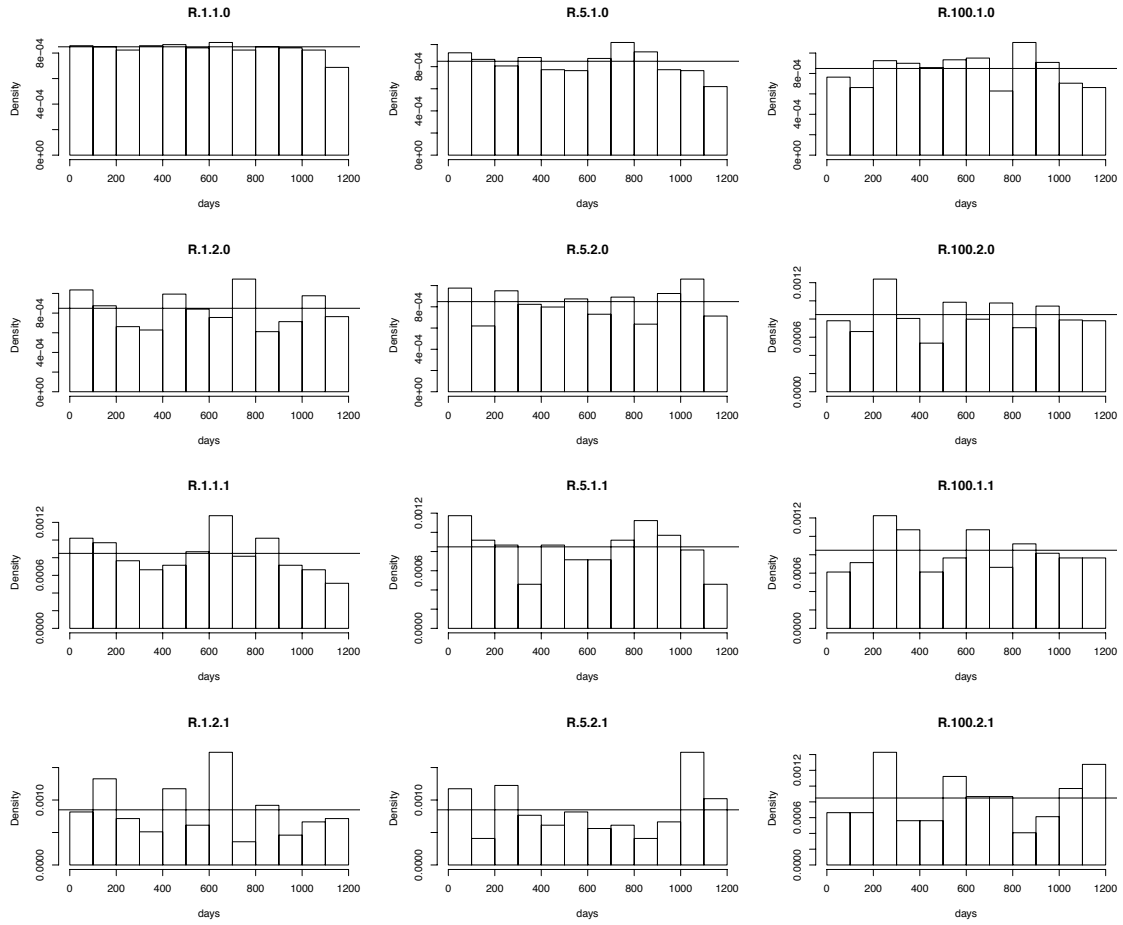


Figure 8. Same as Figure SM7 but for July.

25

30

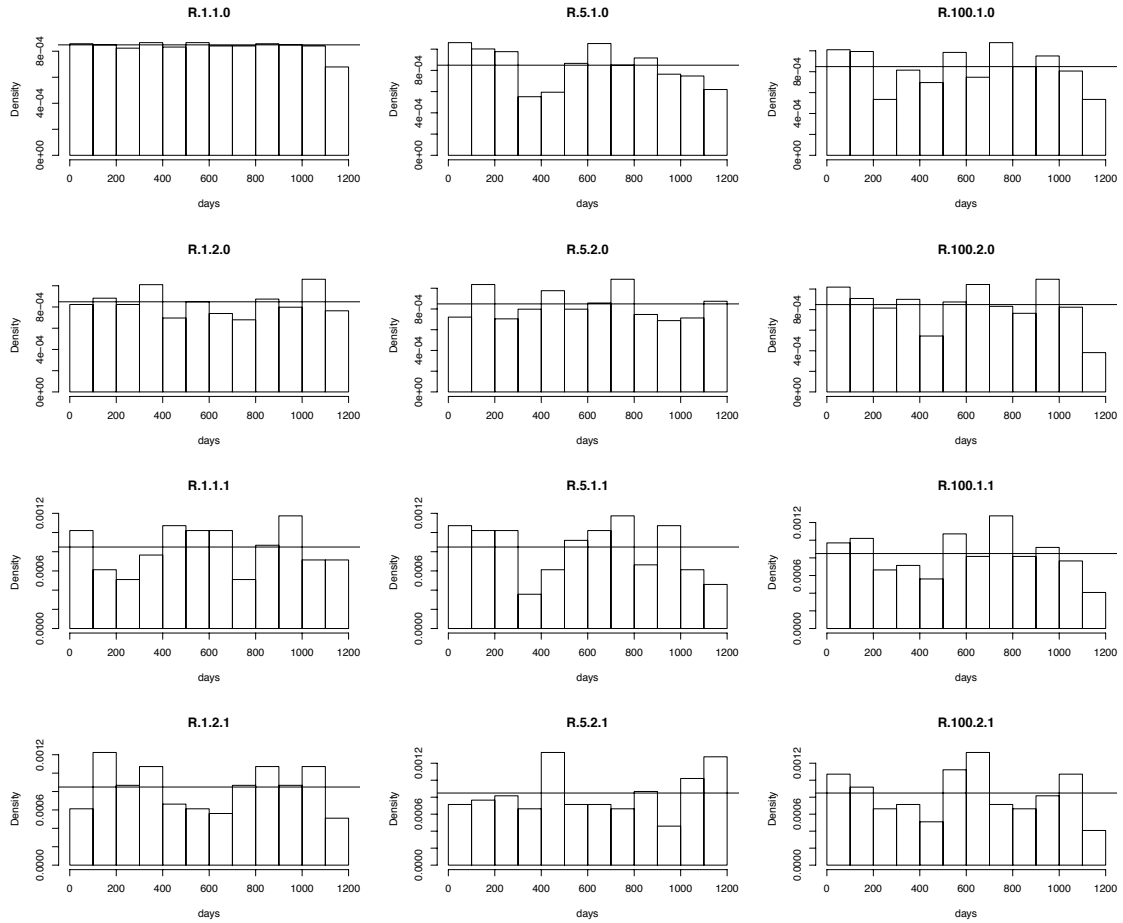


Figure 9. Same as Figure SM7 but for October.

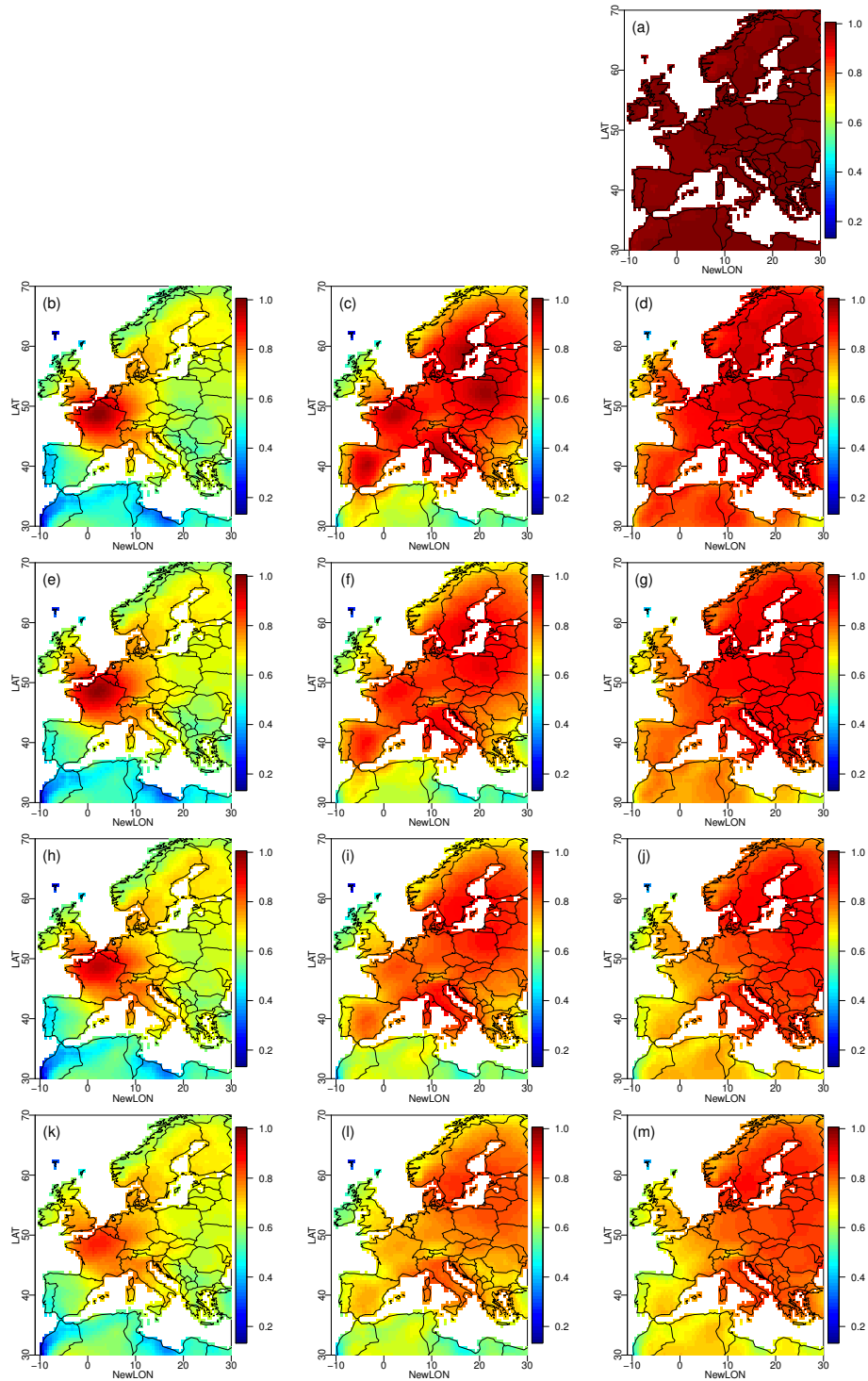


Figure 10. Maps of spearman (rank) correlations calculated for each gridpoint in spring over 1979-2016 between the initial climate model temperature simulations and their corrections by (a) 1d-BC, (b) R.1.1.0, (c) R.5.1.0, (d) R.100.1.0, (e) R.1.2.0, (f) R.5.2.0, (g) R.100.2.0, (h) R.1.1.1, (i) R.5.1.1, (j) R.100.1.1, (k) R.1.2.1, (l) R.5.2.1, (m) R.100.2.1.

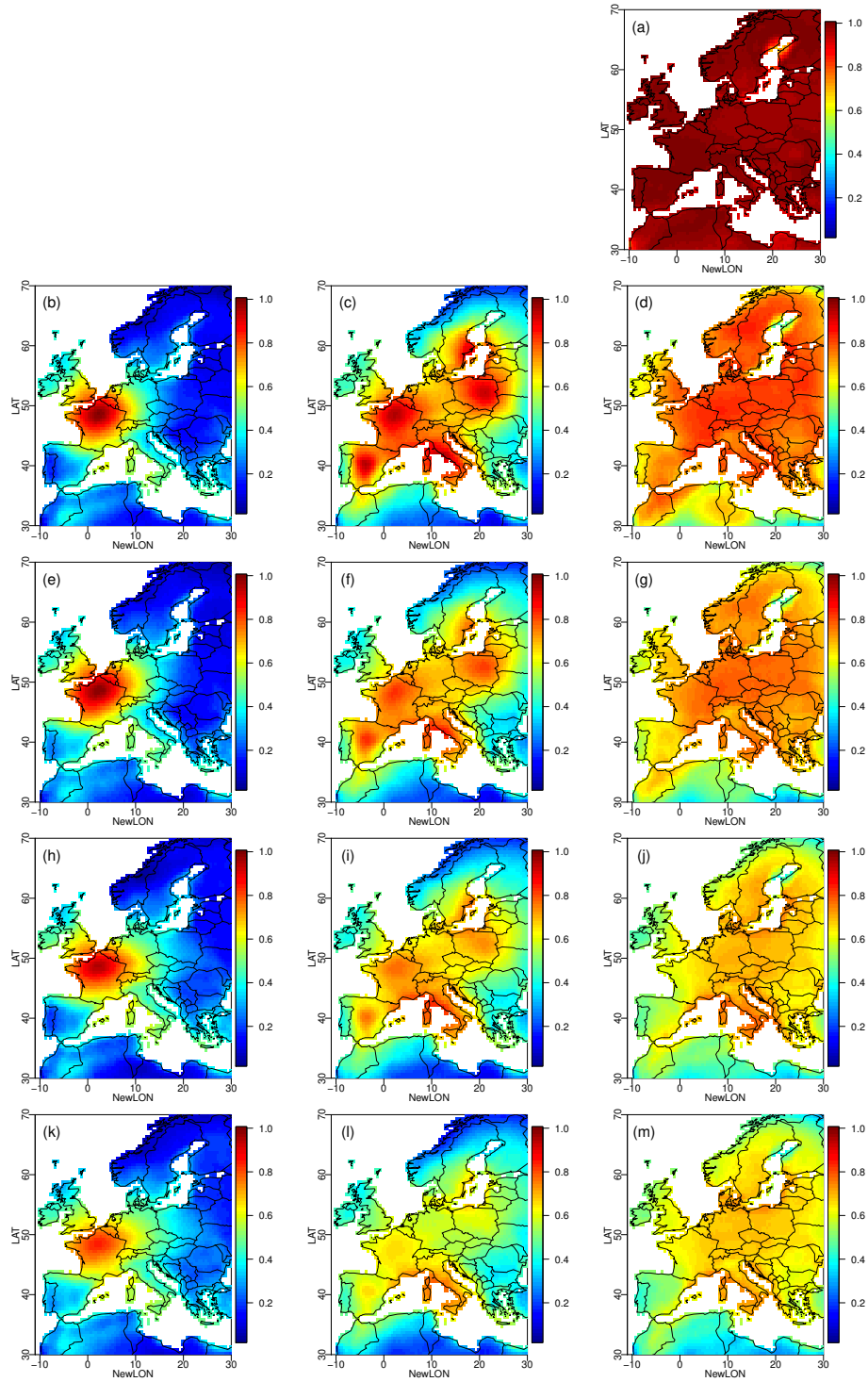


Figure 11. Same as Fig. SM10 but for summer temperature.

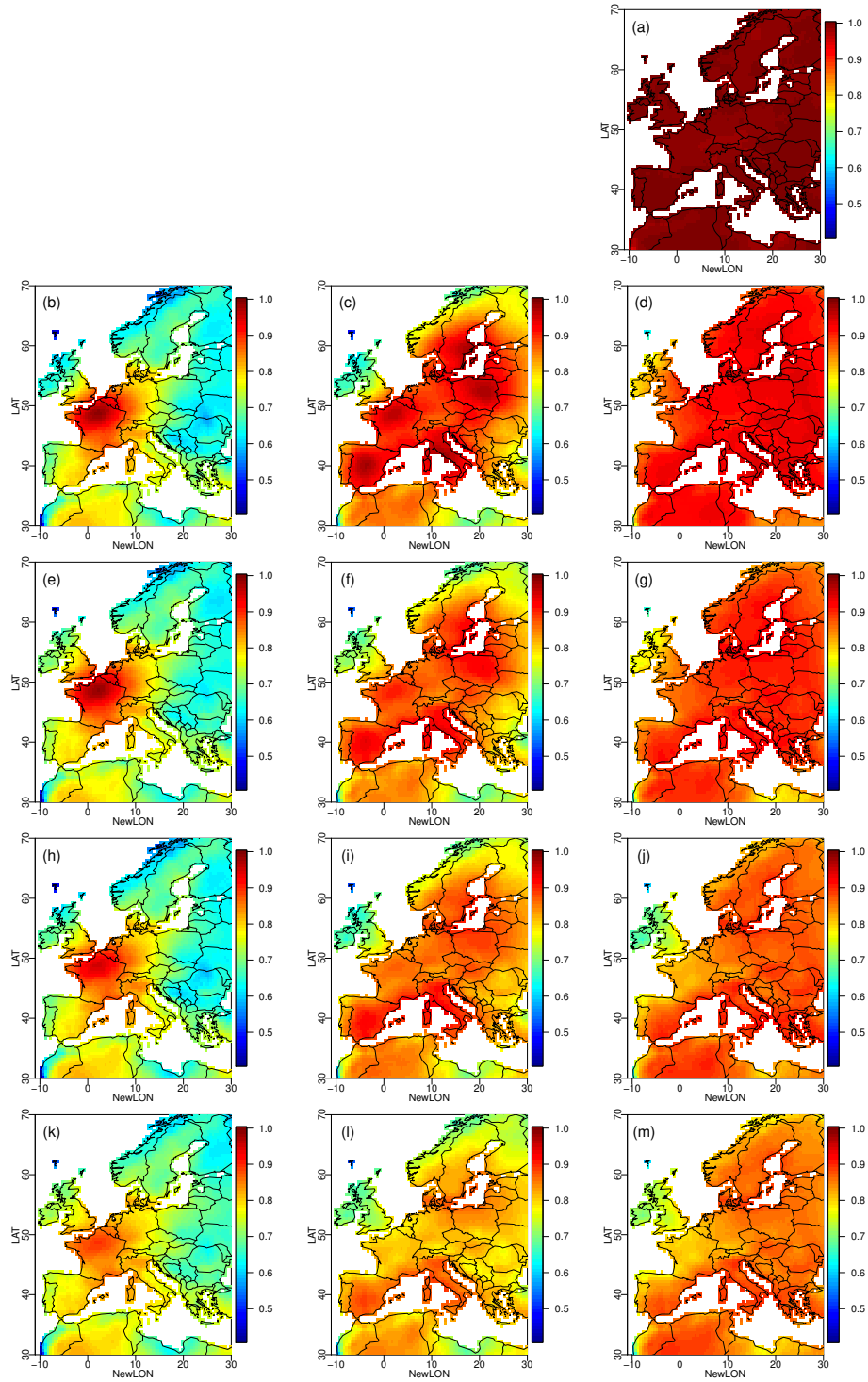


Figure 12. Same as Fig. SM10 but for fall temperature.

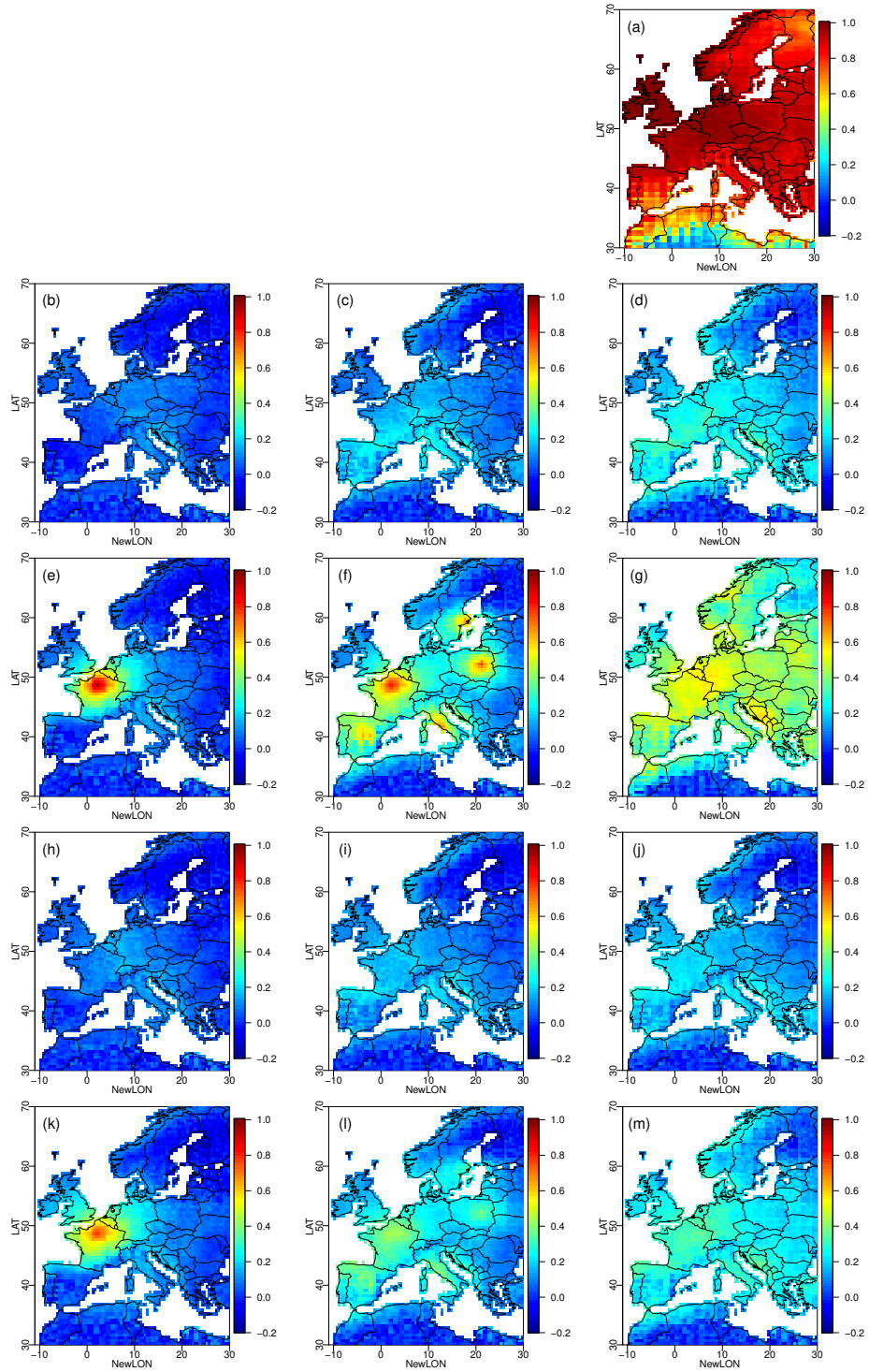


Figure 13. Same as Fig. SM10 but for spring precipitation.

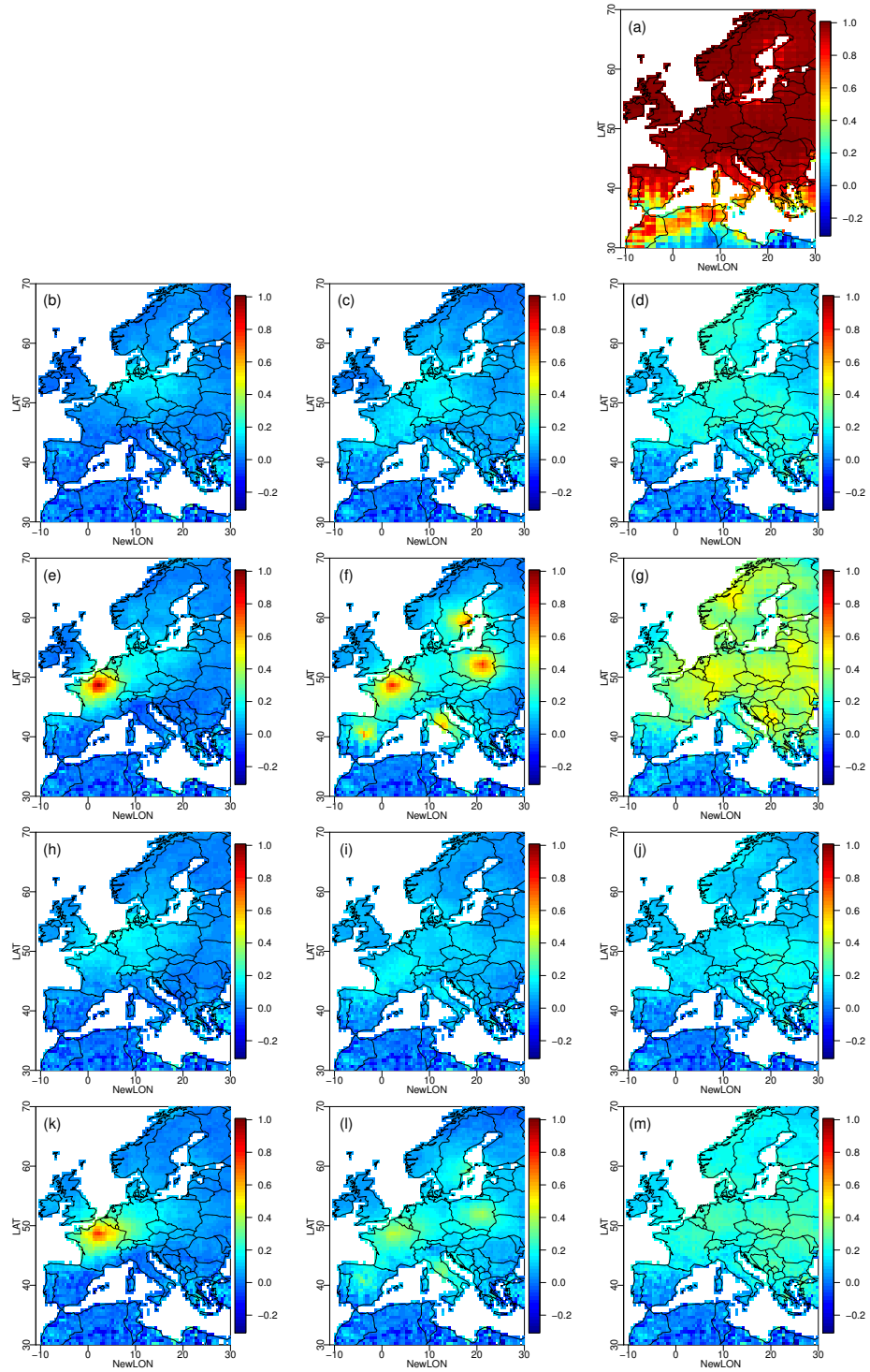


Figure 14. Same as Fig. SM10 but for summer precipitation.

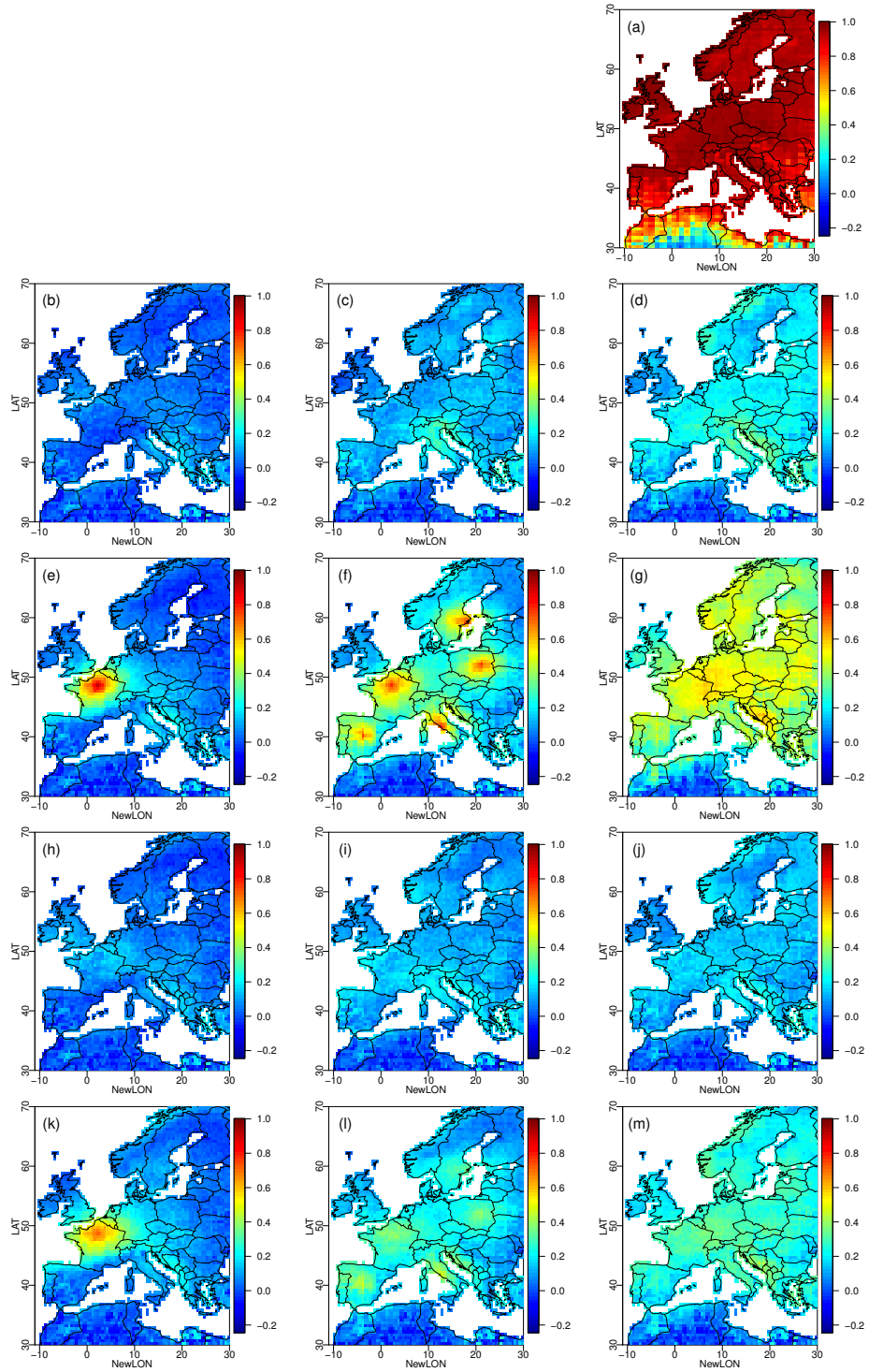


Figure 15. Same as Fig. SM10 but for fall precipitation.

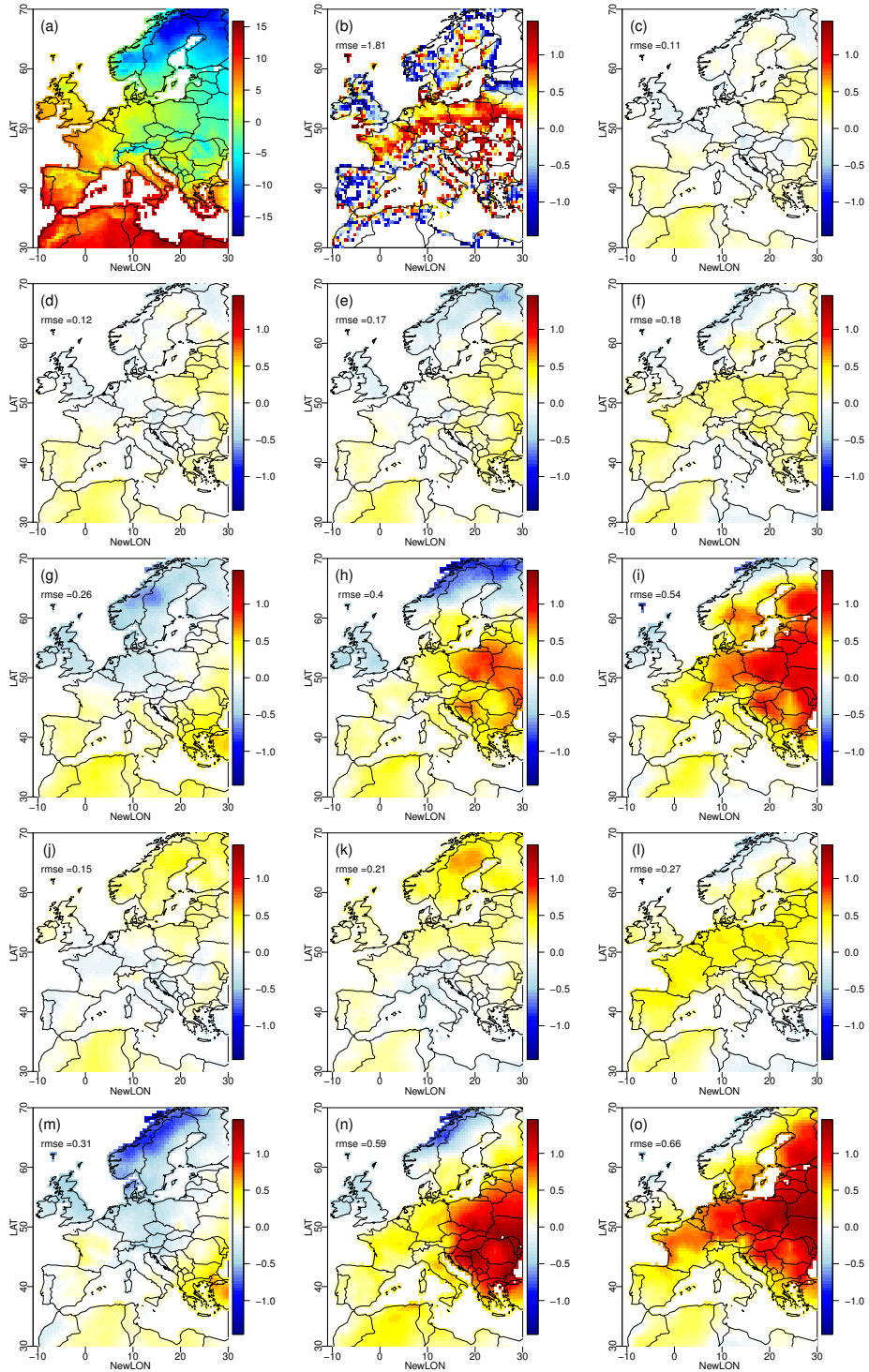


Figure 16. (a) Map of mean temperature (in $^{\circ}\text{C}$) per gridpoint for WFDEI in Winter, 1979-2016; (b-o) Difference of mean temperature wrt WFDEI (i.e., mean(model or BC) minus mean(WFDEI)): (b) raw IPSL simulations, (c) 1d-BC (CDF-t), (d) R.1.1.0, (e) R.5.1.0, (f) R.100.1.0, (g) R.1.2.0, (h) R.5.2.0, (i) R.100.2.0, (j) R.1.1.1, (k) R.5.1.1, (l) R.100.1.1, (m) R.1.2.1, (n) R.5.2.1, (o) R.100.2.1. Note that panels (b-o) have their range censored to facilitate visual comparison.

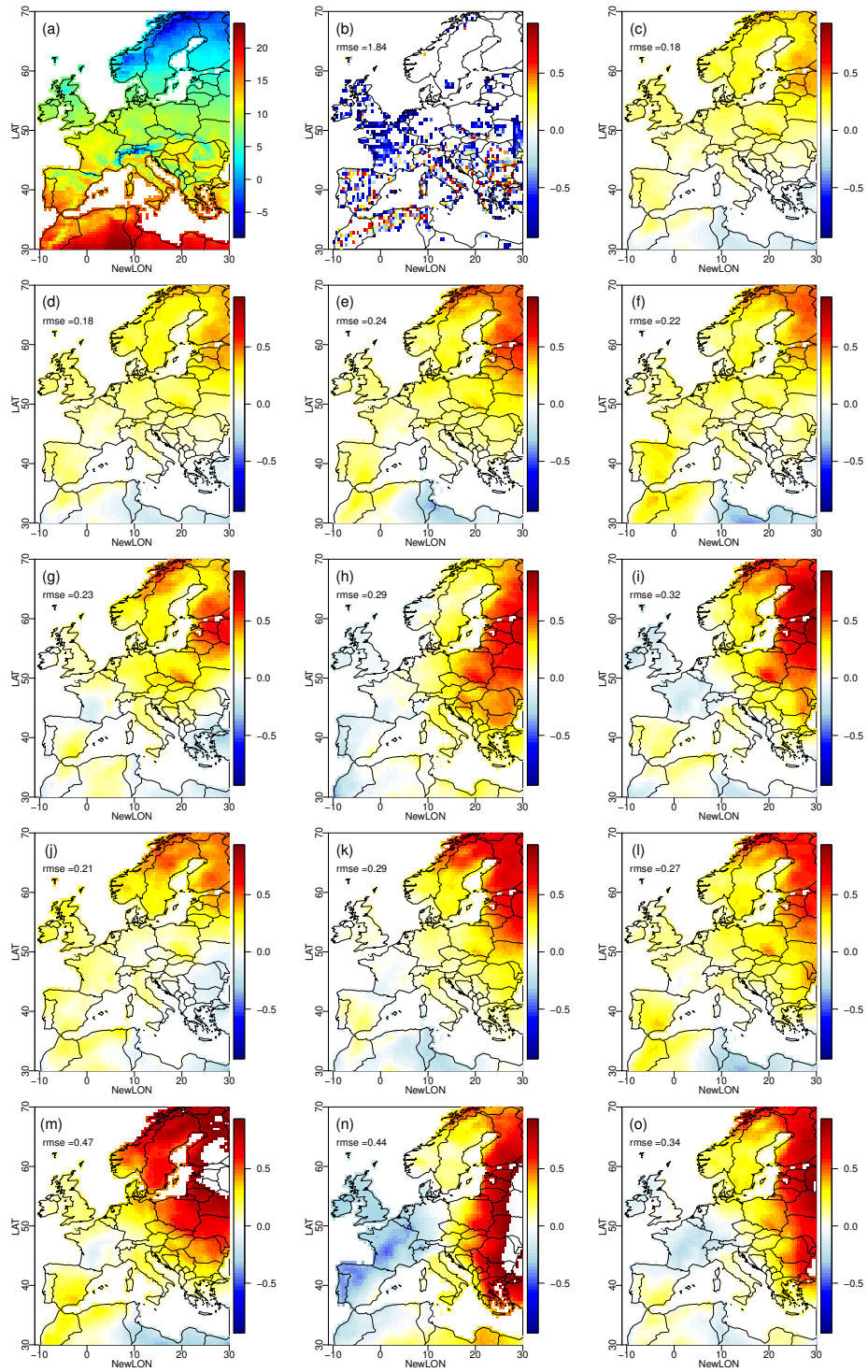


Figure 17. Same as figure SM16 but for spring temperature.

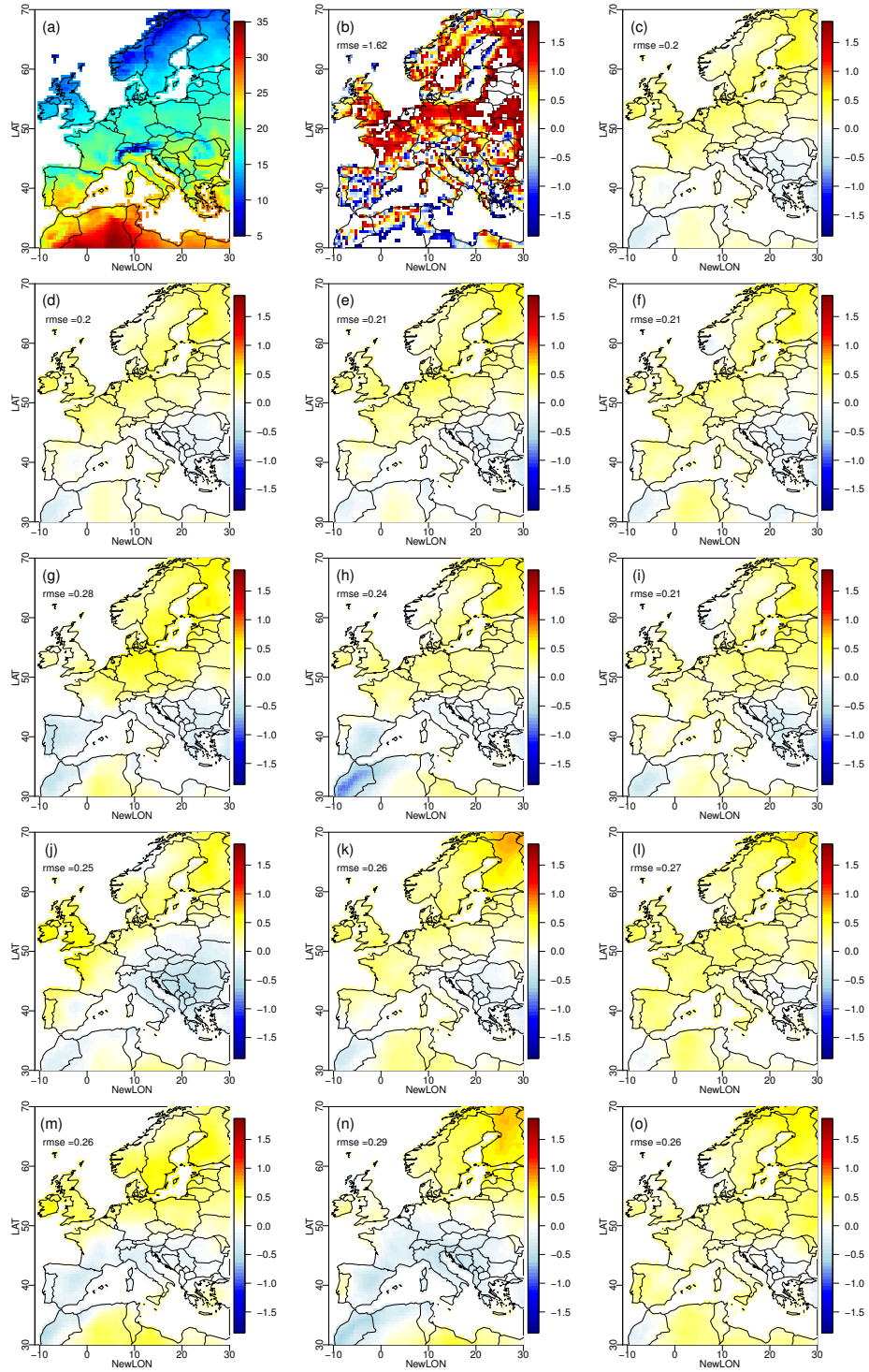


Figure 18. Same as figure SM16 but for summer temperature.

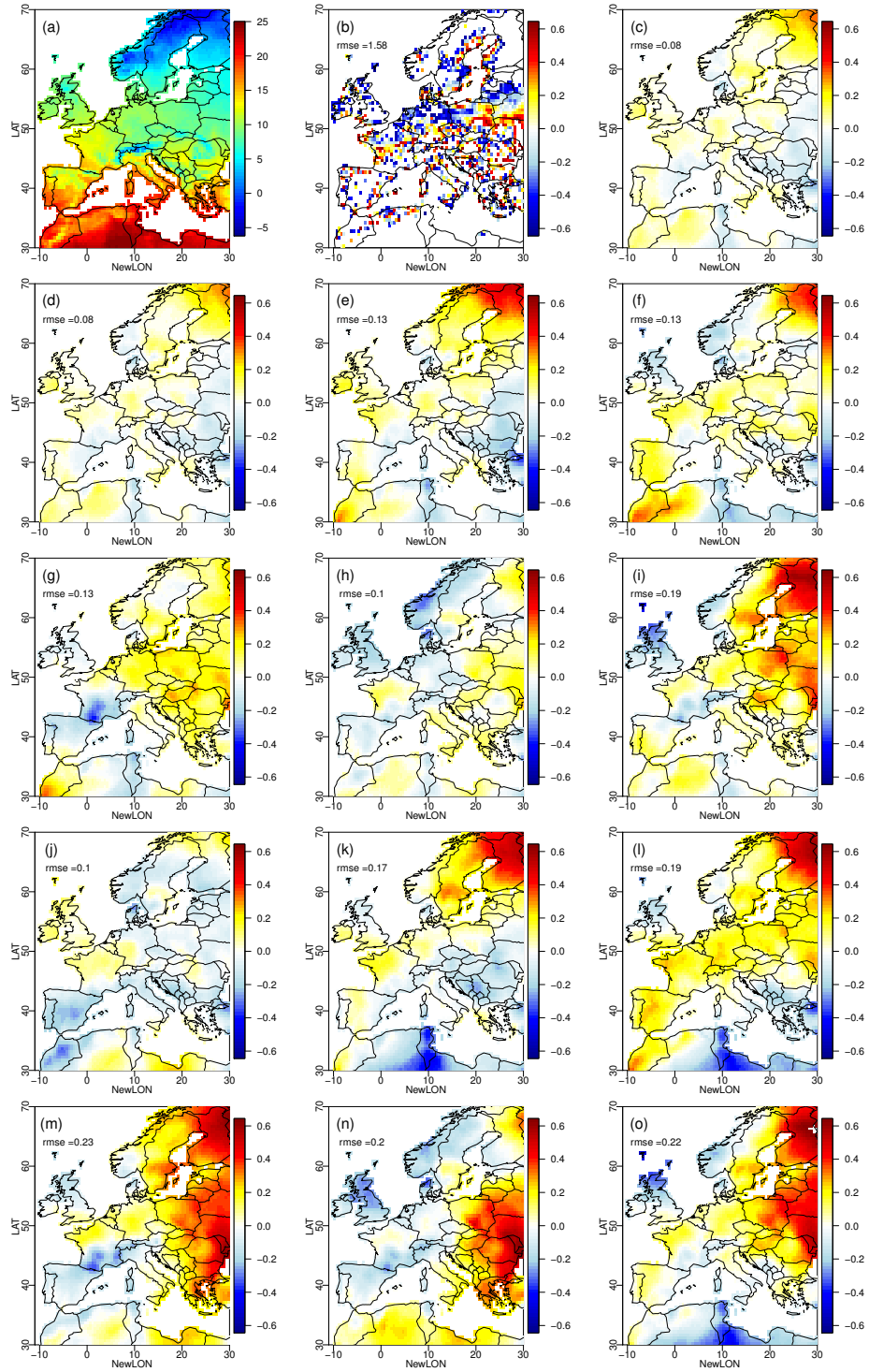


Figure 19. Same as figure SM16 but for fall temperature.

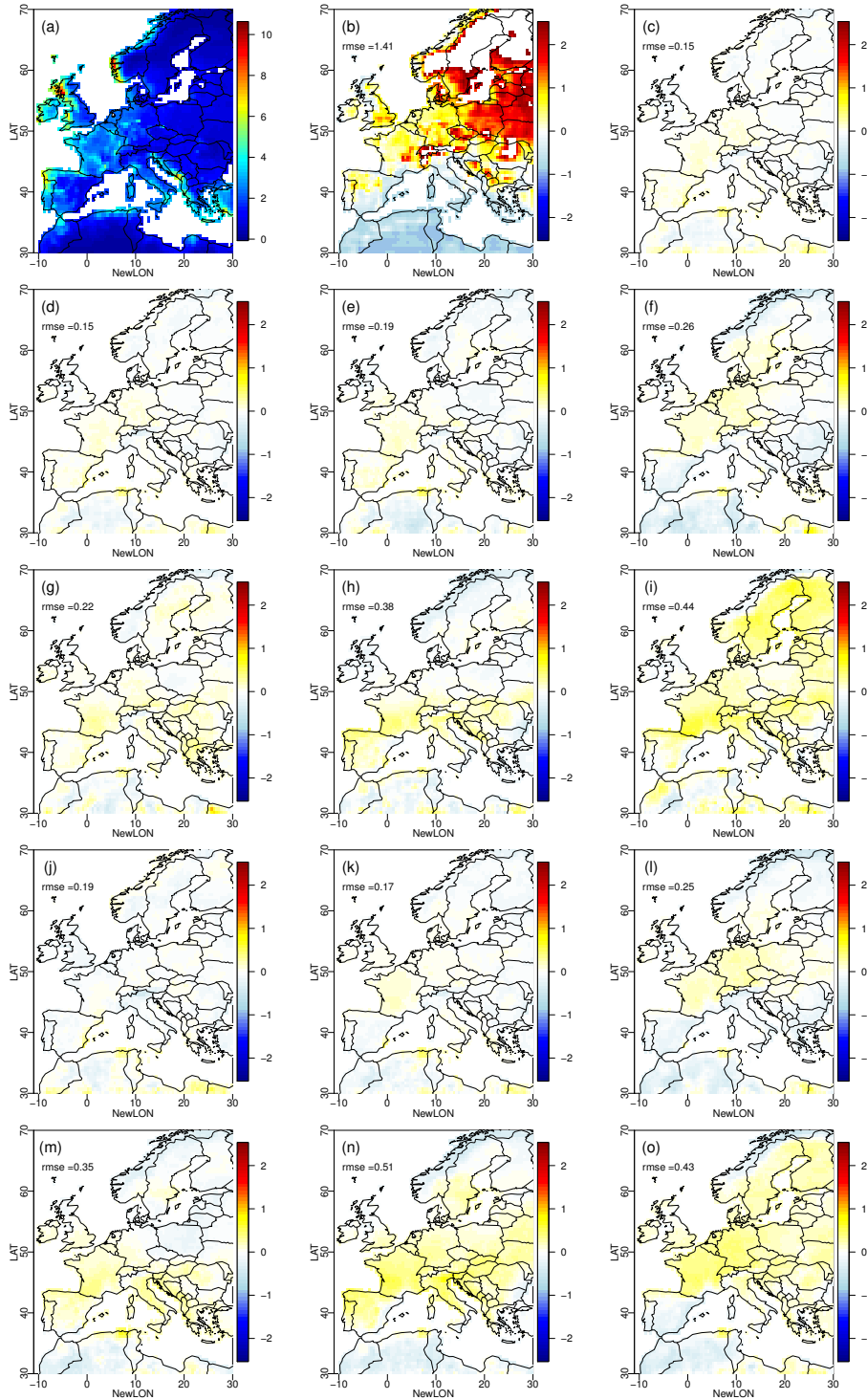


Figure 20. (a) Map of mean precipitation (in mm/day) per gridpoint for WFDEI in Winter, 1979-2016; (b-o) Relative differences of mean temperature wrt WFDEI (i.e., $(\text{mean}(\text{model or BC}) - \text{mean}(\text{WFDEI})) / \text{mean}(\text{WFDEI})$): (b) raw IPSL simulations, (c) 1d-BC (CDF-t), (d) R.1.1.0, (e) R.5.1.0, (f) R.100.1.0, (g) R.1.2.0, (h) R.5.2.0, (i) R.100.2.0, (j) R.1.1.1, (k) R.5.1.1, (l) R.100.1.1, (m) R.1.2.1, (n) R.5.2.1, (o) R.100.2.1. Note that panels (b-o) have their range censored to facilitate visual comparison.

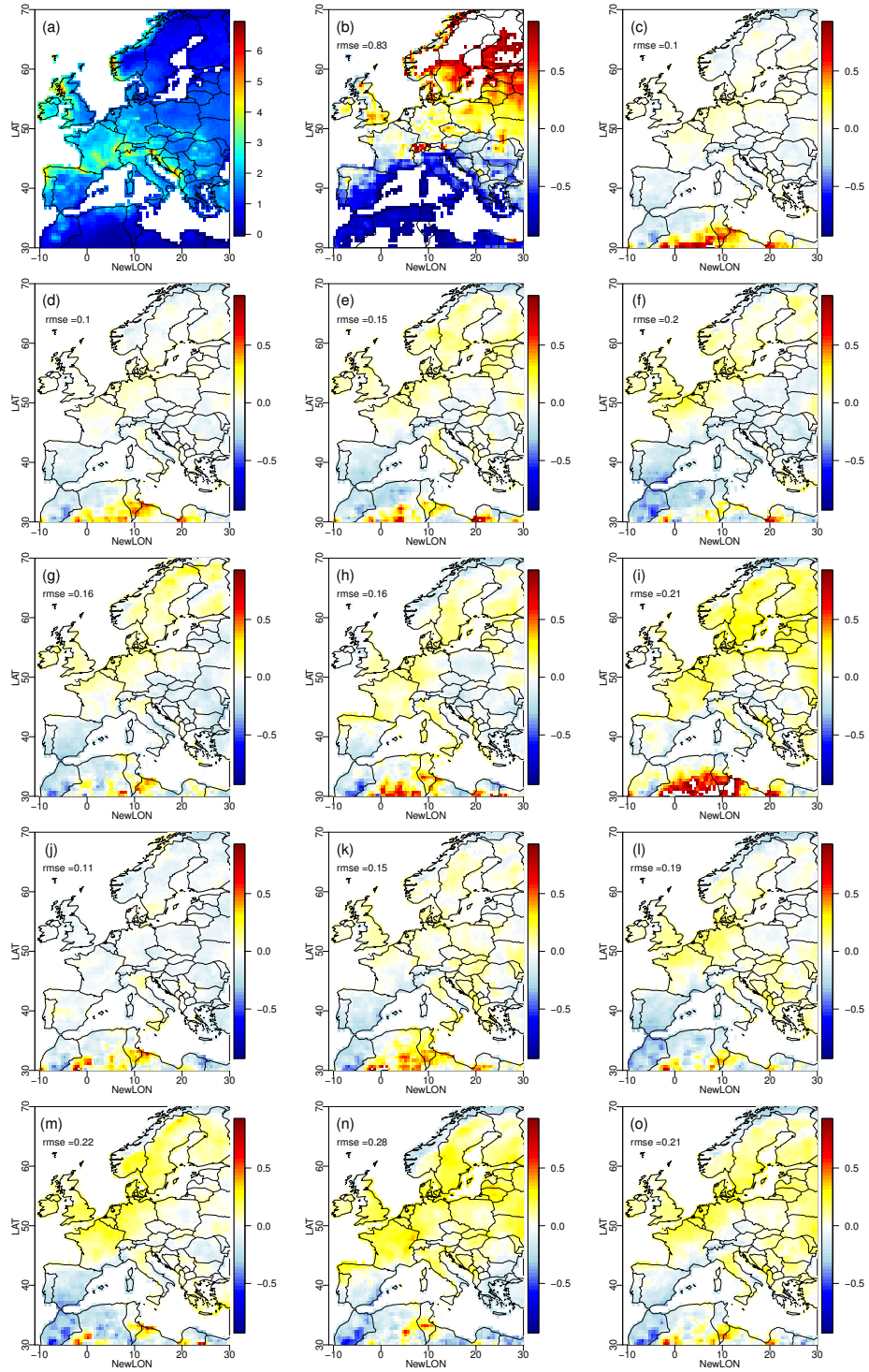


Figure 21. Same as Fig. SM20 but for spring precipitation.

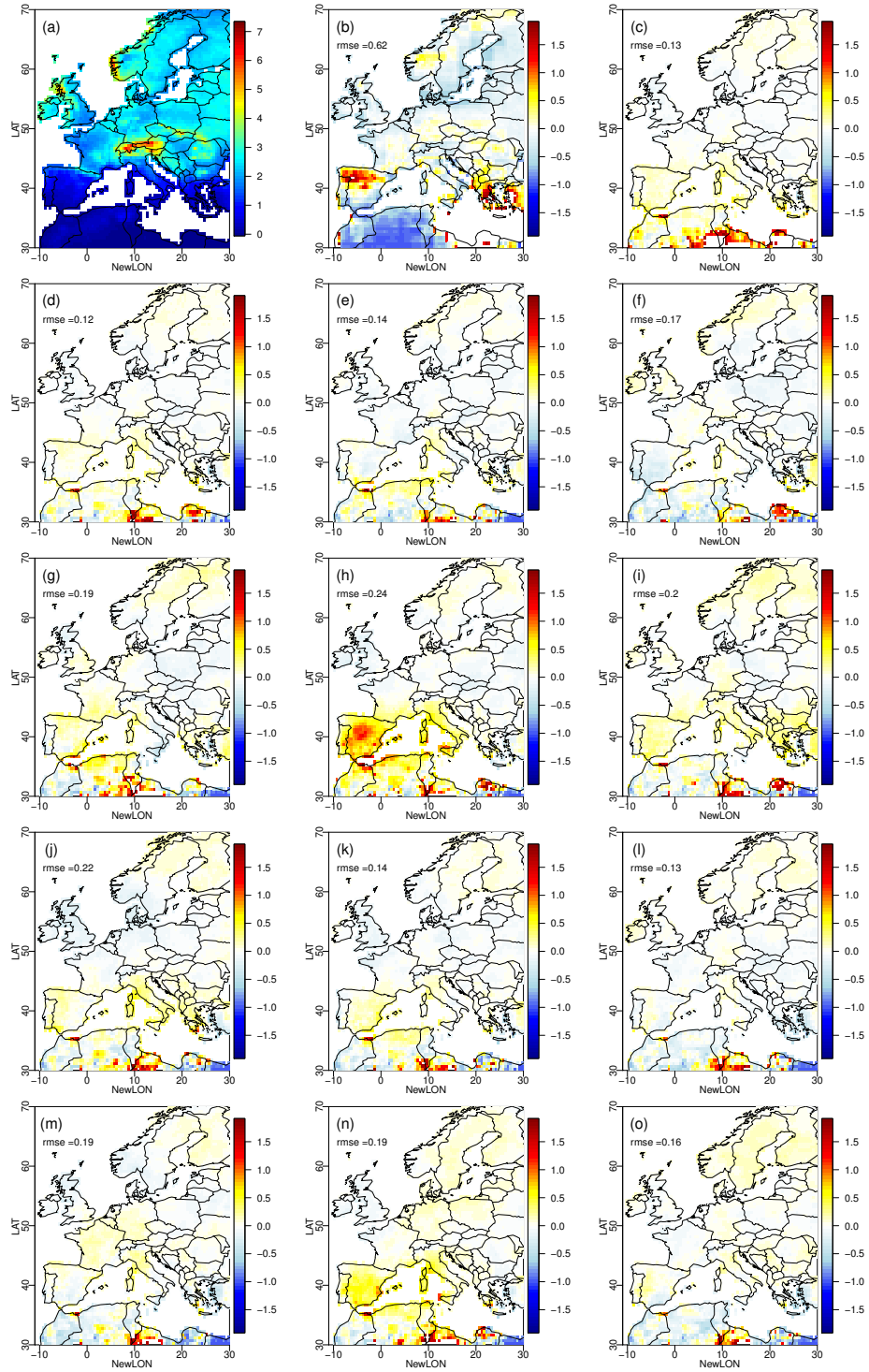


Figure 22. Same as Fig. SM20 but for summer precipitation.

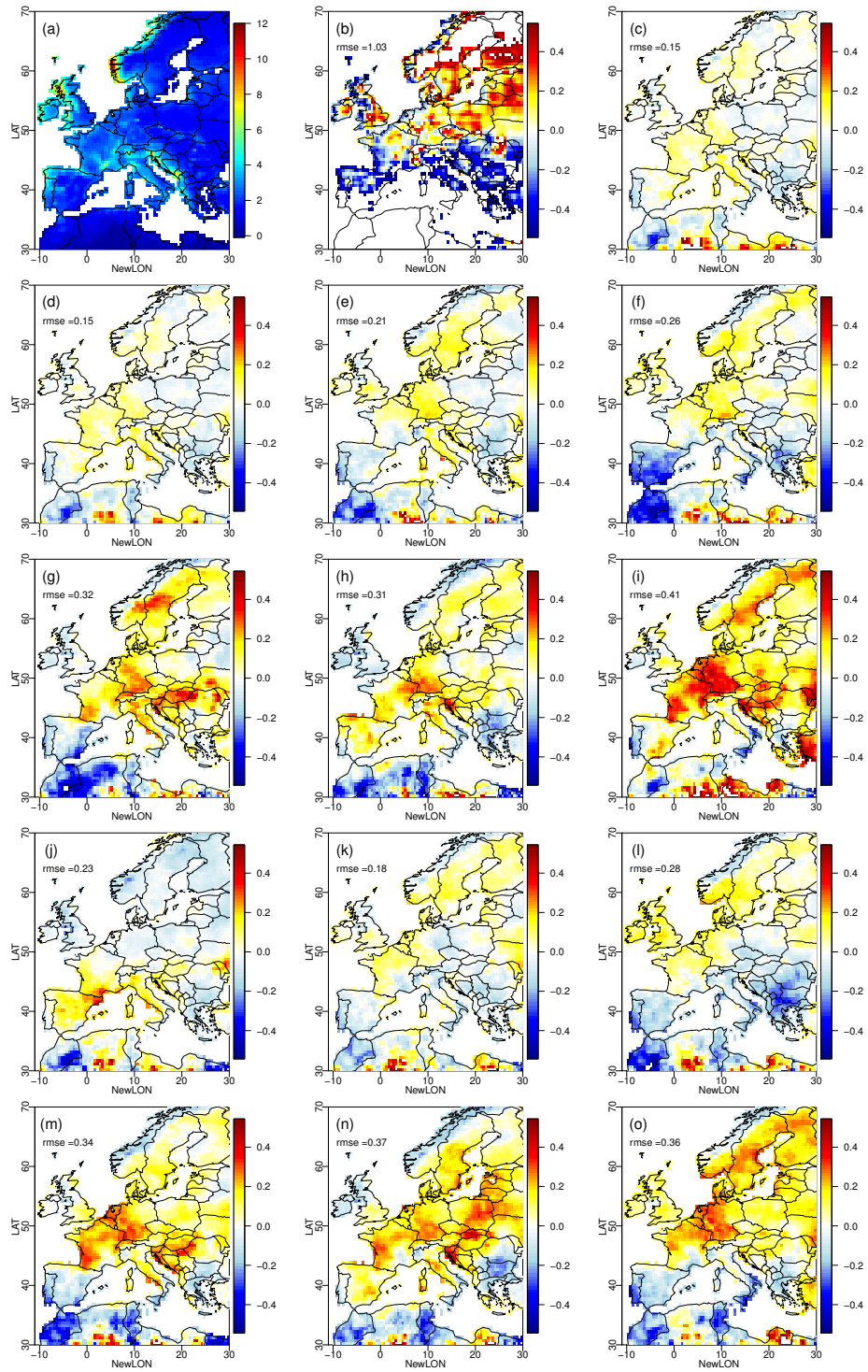


Figure 23. Same as Fig. SM20 but for fall precipitation.

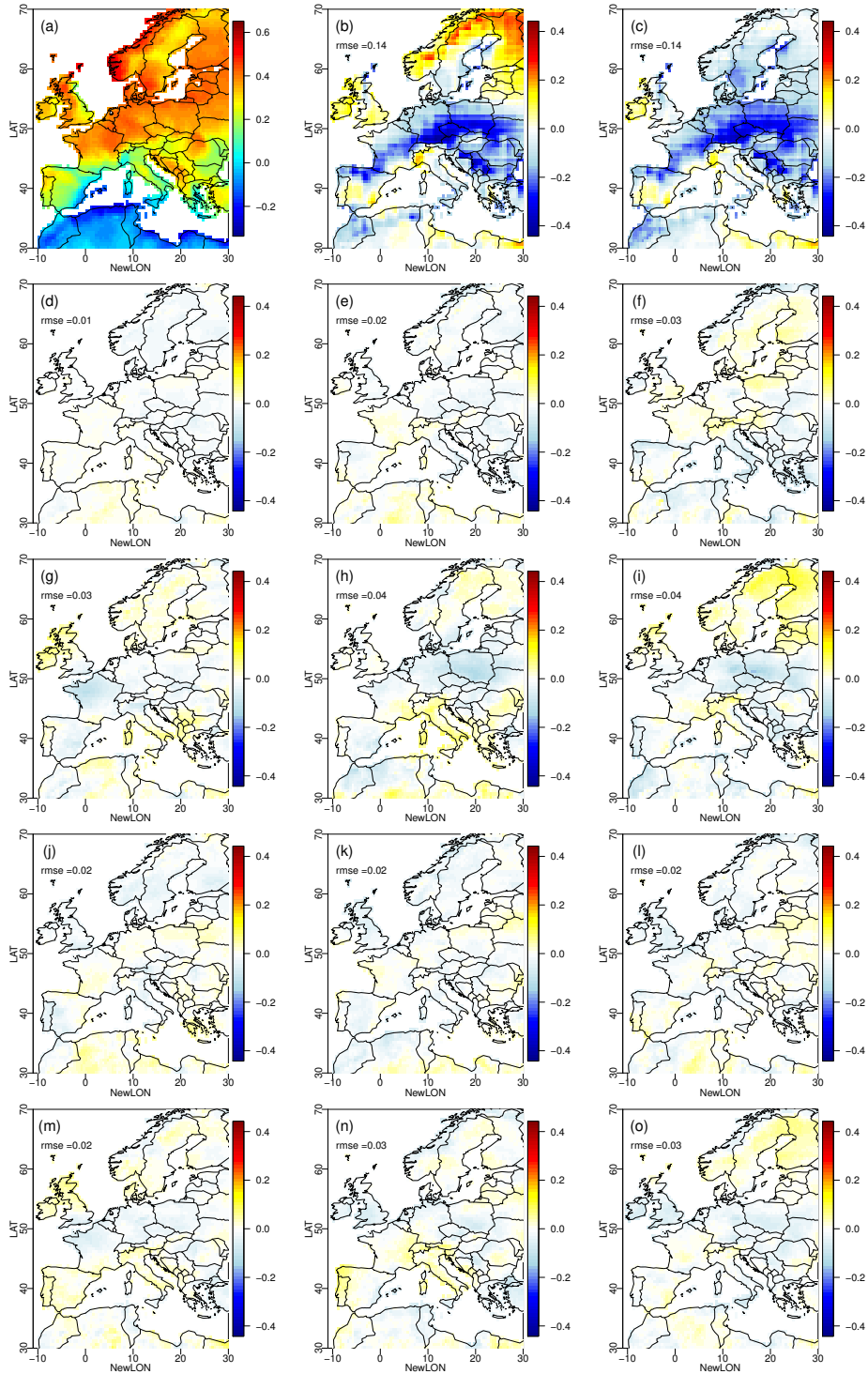


Figure 24. (a) Temperature vs. precipitation correlations for WFDEI in Winter over 1979-2016; (b-m) Differences of correlations between model or corrected data, and WFDEI (i.e., $\text{corr}(\text{model or BC}) - \text{corr}(\text{WFDEI})$): (b) IPSL raw simulations, (c) 1d-bias correction, (d) R.1.1.0, (e) R.5.1.0, (f) R.100.1.0, (g) R.1.2.0, (h) R.5.2.0, (i) R.100.2.0, (j) R.1.1.1, (k) R.5.1.1, (l) R.100.1.1, (m) R.1.2.1, (n) R.5.2.1, (o) R.100.2.1. For (b-o), the RMSE value, computed over the whole domain between WFDEI correlations and those from the model or corrected data, is indicated.

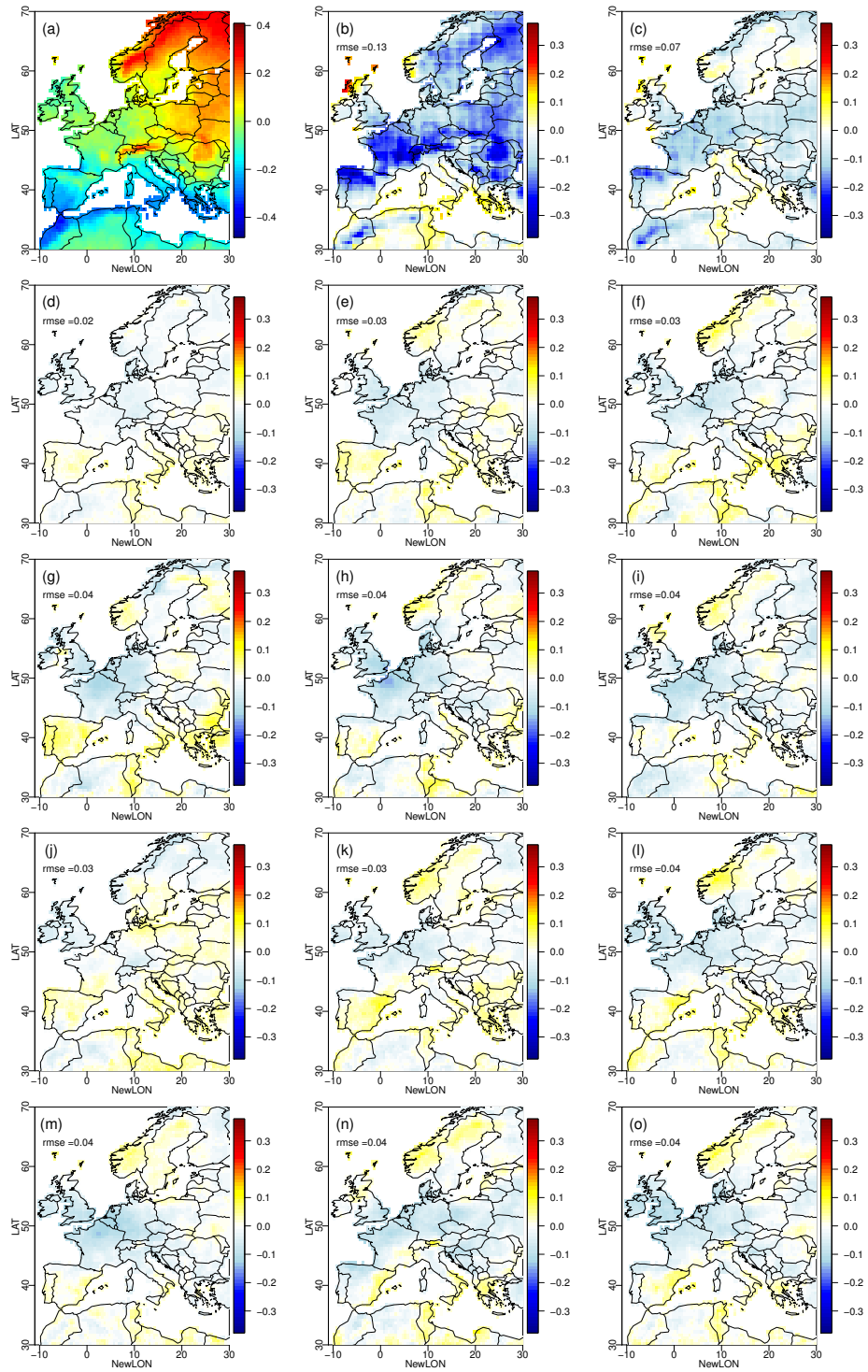


Figure 25. Same as Fig. SM24 but for spring.

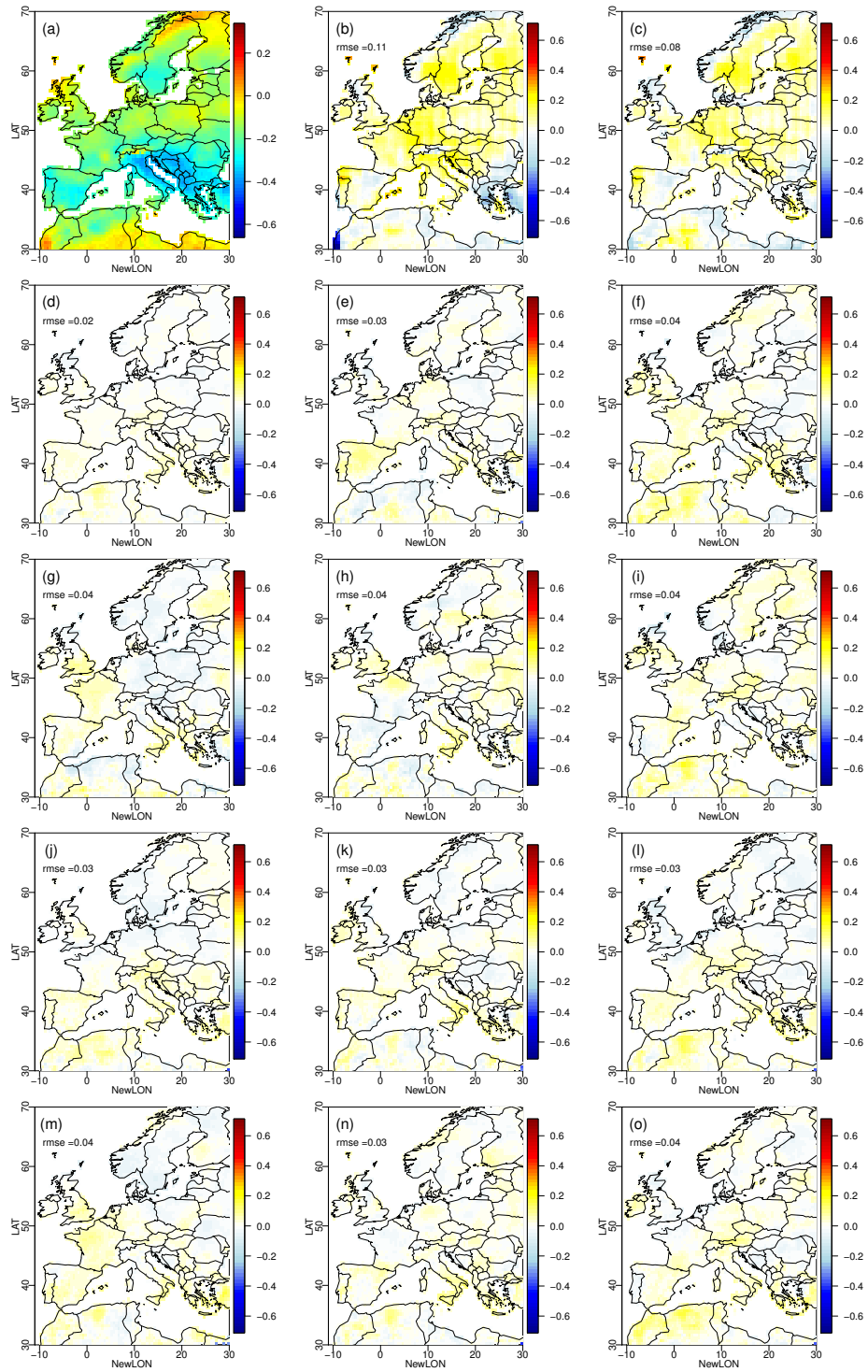


Figure 26. Same as Fig. SM24 but for summer.

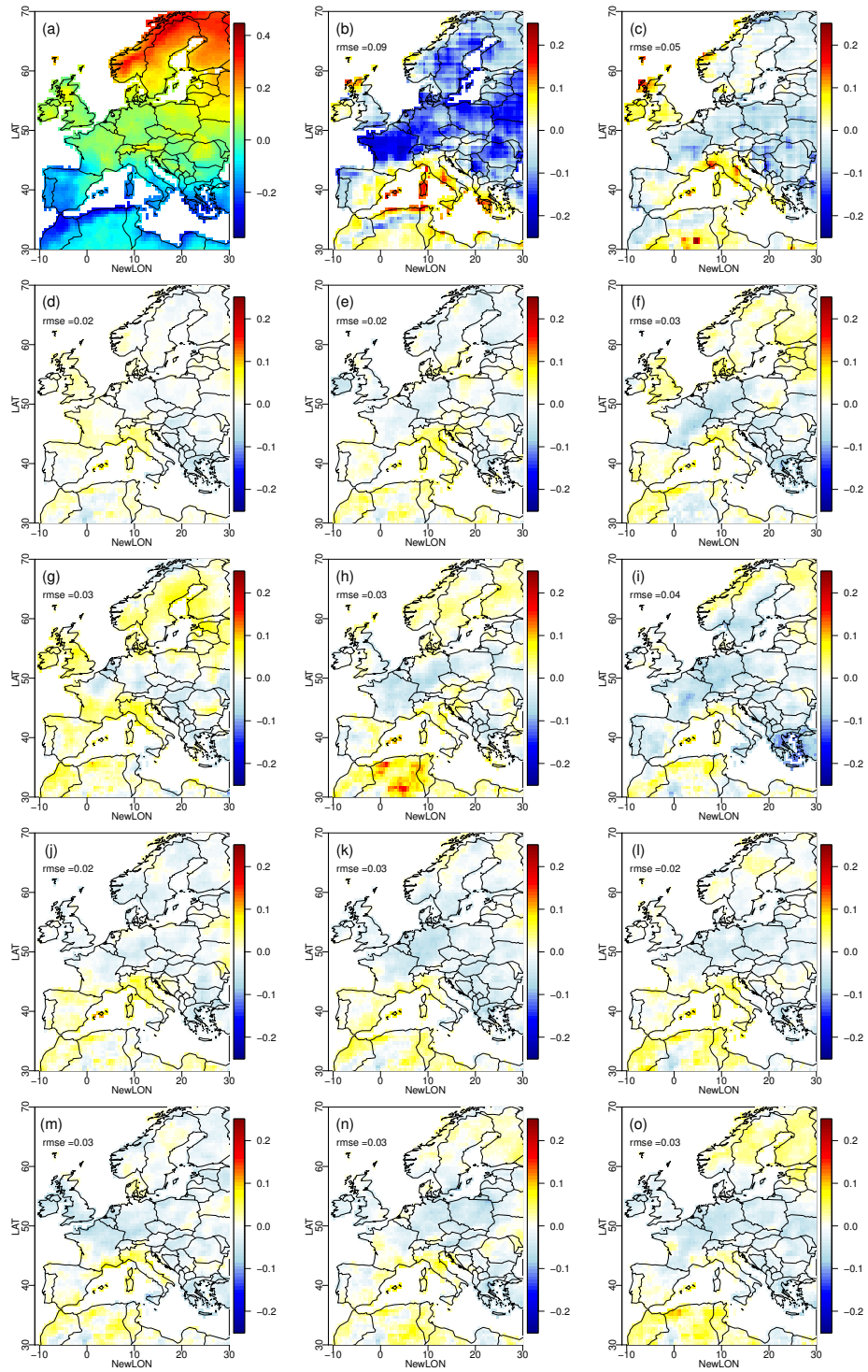


Figure 27. Same as Fig. SM24 but for fall.

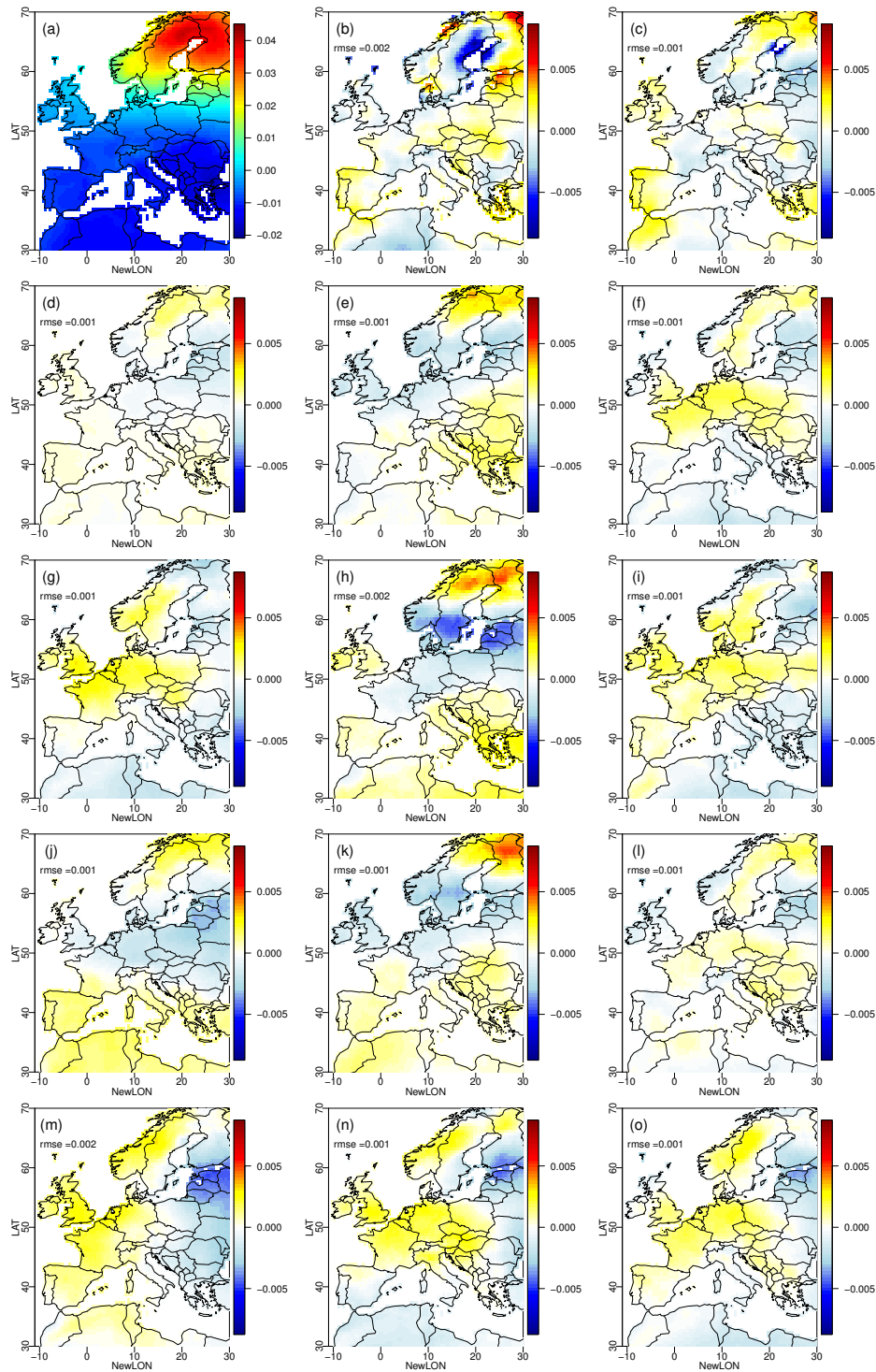


Figure 28. (a) Map of the loading values for the first EOF of temperature for WFDEI in Winter over 1979-2016; (b-m) Differences of loading values for EOF1 between model or corrected data, and WFDEI (i.e., EOF1(model or BC) minus EOF1(WFDEI)). For each panel in (b-m), the RMSE value, computed over the whole domain between WFDEI loading values and those from the model or corrected data, is indicated.

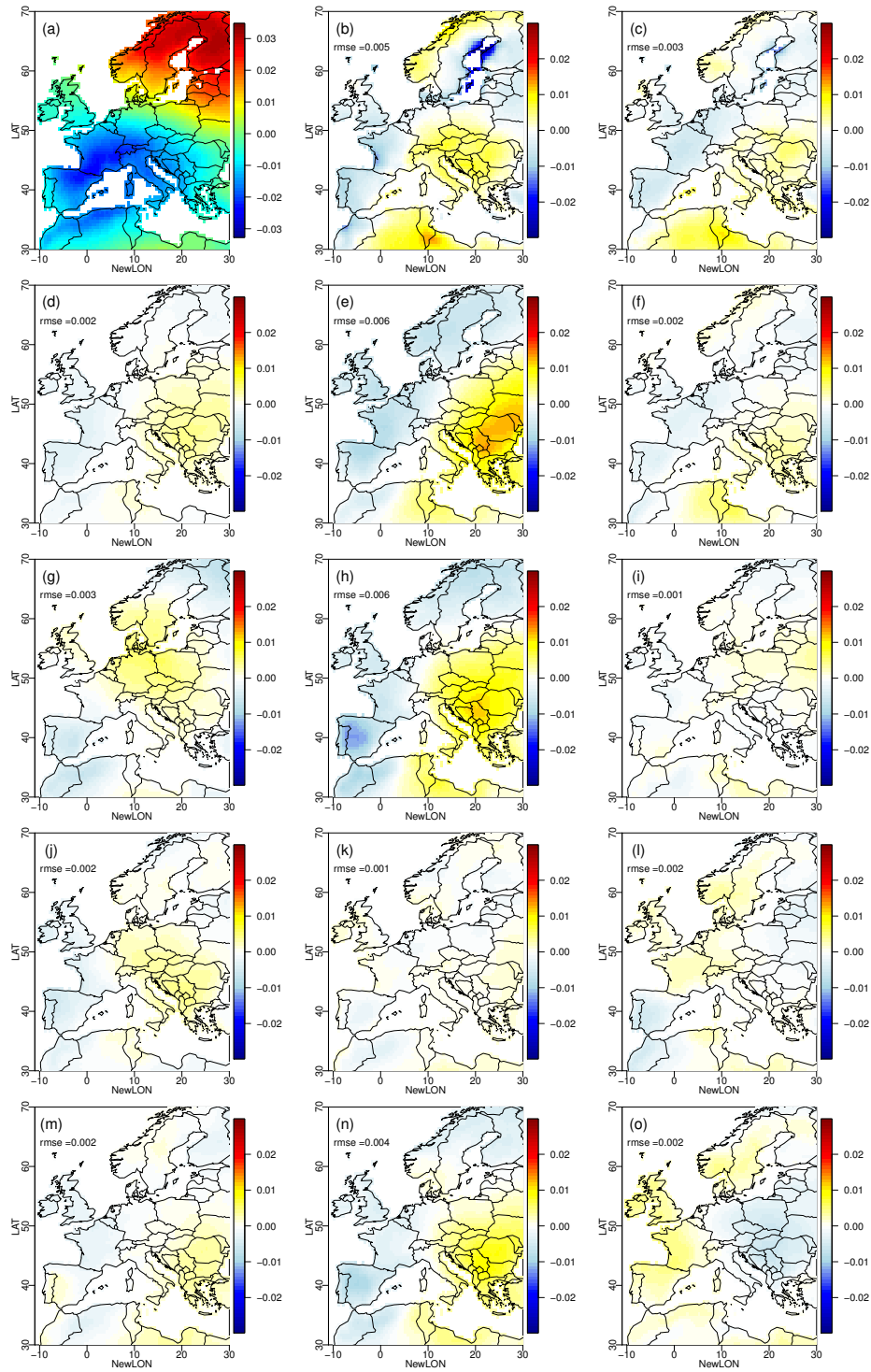


Figure 29. Same as Figure SM28 but for temperature in summer.

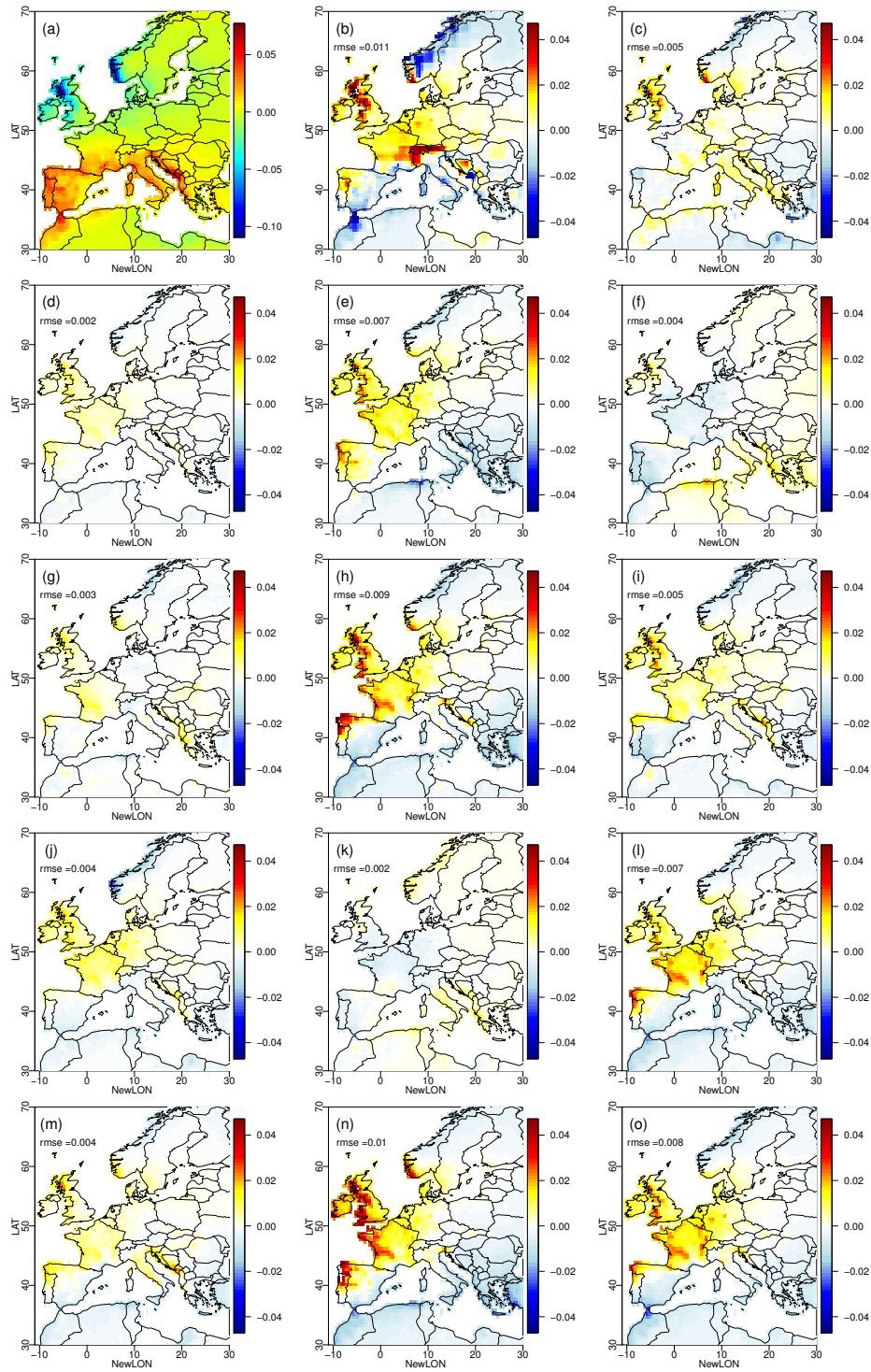


Figure 30. Same as Figure SM28 but for precipitation in winter.

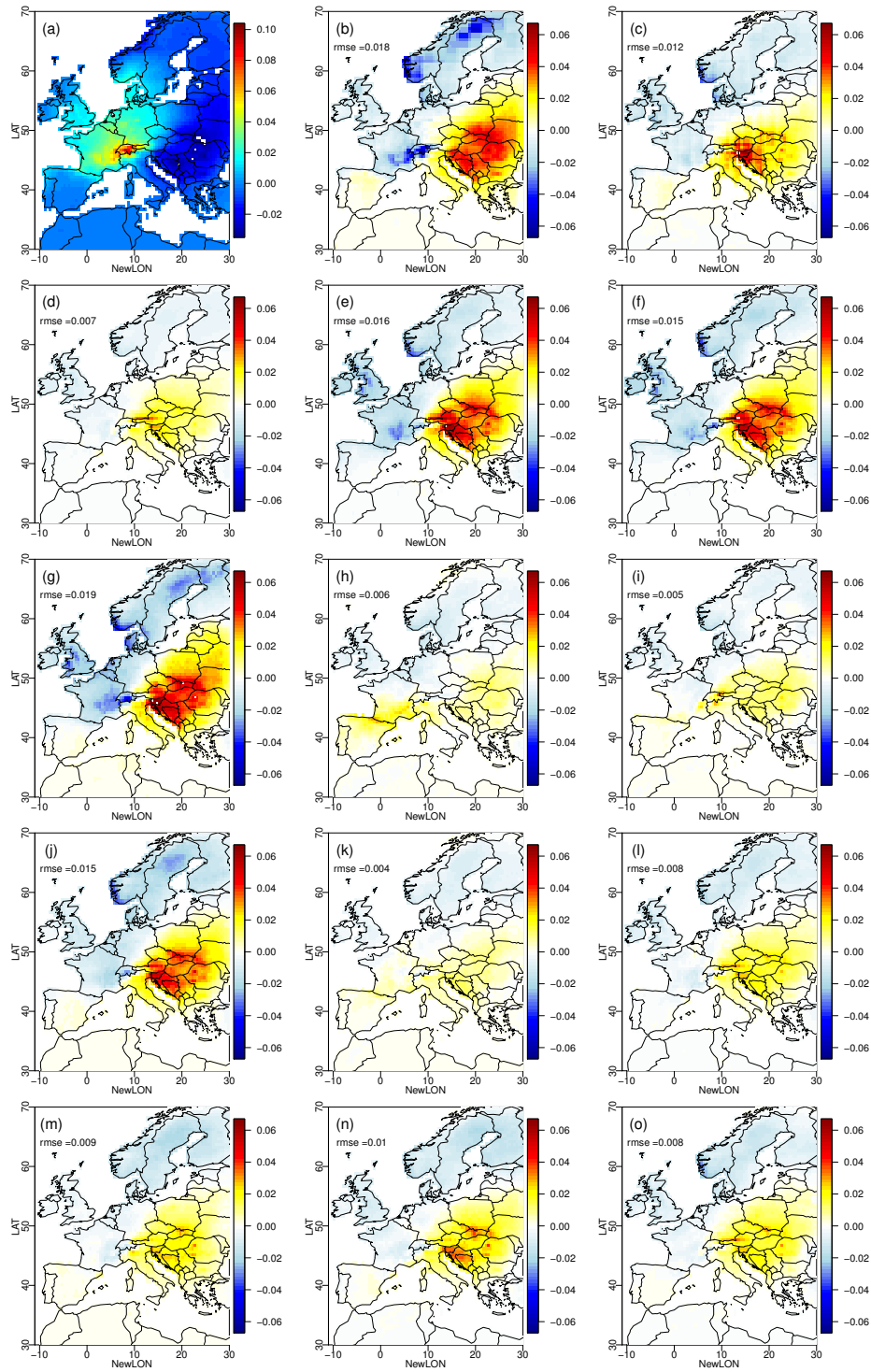


Figure 31. Same as Figure SM28 but for precipitation in summer.